

Variance propagation for density surface models

Mark V. Bravington^{1*}
 David L. Miller^{2*}
 Sharon L. Hedley

Commonwealth Scientific and Industrial Research Organisation Marine Laboratory, Hobart, Australia¹ and Centre for Research into Ecological and Environmental Modelling and School of Mathematics and Statistics, University of St Andrews, St Andrews, Fife, Scotland²

Abstract

Spatially-explicit estimates of population density, together with appropriate estimates of uncertainty, are required in many management contexts. Density Surface Models (DSMs) are a two-stage approach for estimating spatially-varying density from distance-sampling data. First, detection probabilities—perhaps depending on covariates—are estimated based on details of individual encounters; next, local densities are estimated using a GAM, by fitting local encounter rates to location and/or spatially-varying covariates while allowing for the estimated detectabilities. One criticism of DSMs has been that uncertainty from the two stages is not usually propagated correctly into the final variance estimates. We show how to reformulate a DSM so that the uncertainty in detection probability from the distance sampling stage (regardless of its complexity) is captured as an extra random effect in the GAM stage. In effect, we refit an approximation to the detection function model at the same time as fitting the spatial model. This allows straightforward computation of the overall variance via exactly the same software already needed to fit the GAM. A further extension allows for spatial variation in group size, which can be an important covariate for detectability as well as directly affecting abundance. We illustrate these models using point transect survey data of Island Scrub-Jays on Santa Cruz Island, CA and harbour porpoise from the SCANS-II line transect survey of European waters.

Keywords: abundance estimation; distance sampling; generalized additive models; line transect sampling; point transect sampling; spatial modelling;

1 Introduction

Distance sampling is a widely-used method for estimating abundance when detection is imperfect (Buckland et al., 2001), based on encounters along line or point transects. Detection probability (detectability) is estimated using within-encounter data (e.g., perpendicular distance from trackline), by fitting “detection functions” that may involve environmental covariates (e.g., local weather conditions). In traditional stratified distance-sampling, an average animal density is then estimated within each survey stratum—i.e.,

*Joint first author. dave@ninepointeightone.net

some region within which survey coverage is supposed to be uniform—based on the observed encounter rate within that stratum divided by the detectability, and then scaled by the stratum area. Since the abundance estimate is a simple function of statistically independent quantities (encounter rate and detectability), its variance can be estimated straightforwardly.

Instead of using strata, with modern statistical tools it is possible to fit spatially-explicit models of density, where local density is assumed to vary gradually in space (and perhaps also in response to specific environmental covariates, which we here include under the general heading of “spatially-explicit”). Spatially-explicit estimates are advantageous in many situations: when abundance estimates are required across arbitrary sub-regions that do not coincide with survey strata; to reduce bias when coverage is uneven; or when identifying particularly important habitat for conservation, for example.

There are various approaches to actually fitting spatially-explicit models. The general idea, as in the stratified case, is that the expected local encounter rate is the product of local detectability and local density, but with both factors now potentially depending on local spatial and/or environmental covariates. Here we consider specifically Density Surface Models (DSMs; Hedley and Buckland, 2004; Miller et al., 2013), which take a two-stage approach. The first stage is to estimate detectability using a detection function model; any standard or bespoke model could be used (see Section 2). In the second stage, the encounter rate data are fitted to location/environmental covariates using a GAM, specifically the “basis-and-penalty” formulation of GAMs in Wood (2017) in which smoothers are represented via random effects. The estimated detectabilities for each segment of search effort are easily accommodated in the GAM (technically, as offsets to the linear predictor; see below), and the range of smoothers and interactions that can be fitted in is very wide.

Splitting the analysis into two stages is appealing partly because existing domain-specific software and diagnostic expertise can be applied as-is to each stage separately, and partly because it avoids any need to write inevitably complicated code that incorporates two individually-complex aspects. It is also straightforward to produce a point estimate of abundance for any desired sub-region straight from the fitted GAM. However, when detectability and density both vary spatially, the problem is what to do about variance given that GAMs do not intrinsically “understand” the notion of uncertainty in their offset.

In this paper, we show how statistical uncertainty about detectability can in fact be accommodated painlessly within standard GAM software. Our approach is to first fit the detection function as usual, but then to rewrite the fitted detection function log-likelihood as a quadratic approximation centred on its point estimates, and to incorporate the uncertainty about the detection function parameters via random effects in the second-stage GAM. This fits directly and automatically into the Wood/Wahba formulation of a GAM, whereby a smooth surface is described by a set of coefficients treated as random effects; thus, the machinery for handling random effects in general is already built into the `mgcv` software used in Miller et al. (2013)’s DSM code. This amounts to re-fitting the detection function model (or a good approximation to it) at the same time as fitting the GAM. We retain the benefits of two-stage modeling, but all the uncertainty about detectability as well as density is now captured in the usual GAM outputs. The re-fitted detection function model should not differ greatly from the original fit, and we use this idea to propose a diagnostic for overall model specification issues.

Following a summary of DSMs and notation in Section 2, we present our new formu-

lation in Section 3, including variance computation and diagnostics. Section 4 comments on problems with existing approaches to variance propagation in DSMs. In Section 5, we extend the formulation to cover DSMs where group size varies spatially and affects detectability (a common situation with whales and dolphins). Section 6 gives examples of the variance propagation method and the group size model. Some discussion is given in Section 7, including possible generalizations.

2 Density surface models

In distance sampling observers move along a set of survey lines or between points, counting (groups of) animals, recording distances from the centre line or centre point to the observed groups (or their cues, such as blows for cetaceans or calls for birds), the size of each detected group and potentially other covariates that may effect detectability.

To fully describe the DSMs in this paper, we distinguish four different classes of variable.

1. Density covariates, x , vary in space and potentially affect local animal abundance: e.g., latitude and depth. They are required for prediction and fitting, and are assumed known across the entire region of interest.
2. Effort covariate(s), z , affect detection probability: e.g., sea conditions measured on the Beaufort scale, or observer identity. They are assumed known along each transect, but not necessarily in unsurveyed areas.
3. Individual covariates, g , that affect detection probability and are a persistent property of each group (independent of whether the group is observed or not) during its window of observability: e.g., size (number of animals), and perhaps behaviour. Here g is assumed known for each observed group (see Discussion). The random variable G varies from one group to the next, and its statistical distribution $F_G(g; x)$ may vary spatially. $F_G(g; x)$ may have a direct effect on abundance (via the mean group size), as well as on detection probability, in which case it is also necessary to estimate certain properties of $F_G(g; x)$ such as its local mean.
4. Observation variables, y , which are random properties of one observation on one group: e.g., perpendicular distance between the group and the sampler. In certain settings, y may contain other elements. For example, in a multi-observer-platform survey (e.g., MRDS; Borchers et al., 1998), y might also include which of the active observers saw the group; in a cue-based setting, y might include the bearing between sighting and observer.

These classes are assumed to be mutually exclusive; overlaps can lead to fundamental problems for distance sampling which we do not address here (e.g., non-uniform animal distribution within the sample unit; Marques et al., 2012). The distinction between *individual* and *effort* covariates is often glossed over but they have rather different implications for abundance estimation (see below).

In the first stage of DSM, the detection function $\pi(y|\theta, z, g)$, which involves unknown parameters θ as well as z and g , describes the probability of making an observation at y . The parameters θ are usually estimated by maximizing this log-likelihood across observations s :

$$l(\boldsymbol{\theta}) = \sum_s \log_e \left(\frac{\pi(y_s | \boldsymbol{\theta}, z_{t_s}, g_s)}{p(\boldsymbol{\theta}; z_{t_s}, g_s)} \right) \quad (1)$$

where t_s is the transect containing sighting s . Here p is the overall detection probability for a group, defined by

$$p(\boldsymbol{\theta}; z, g) = \int \pi(y; \boldsymbol{\theta}, z, g) dF_Y(y)$$

where F_Y is the distribution function of y . In standard distance sampling where y consists only of perpendicular distance, F_Y is uniform between 0 and some fixed truncation distance, beyond which observations are discarded. This formulation encompasses a wide range of models, including multiple covariate distance sampling (MCDS; Marques and Buckland, 2003) with z and g , multi-observer mark-recapture distance sampling (MRDS; Borchers et al., 1998), and cue-based “hazard probability models” (Skaug and Schweder, 1999).

The second part of DSM models the local count of observations via a GAM to capture spatial variation in animal density. This allows us both to estimate abundance within any sub-region of interest, and to compensate as far as possible for uneven survey coverage (whether by design, or by virtue of field logistics and weather conditions). Since line transects are generally very long in comparison to their width and therefore contain a range of density and density covariate values, we divide transects into smaller segments, which are the sample units for GAM (in which case the subscript t_s above refers to segments rather than transects). Point transects are left as-is; we use the term “segments” from now on to refer to both points and line segments, without loss of generality. Environmental covariates are assumed not to change much within each segment. The relationship between counts n_i per segment i and density covariates x_{ik} is modelled as an additive combination of smooth functions with a log link:

$$\mathbb{E} [n_i | \boldsymbol{\beta}, \boldsymbol{\lambda}, p(\hat{\boldsymbol{\theta}}; \mathbf{z}_i)] = a_i p(\hat{\boldsymbol{\theta}}; \mathbf{z}_i) \exp \left(\beta_0 + \sum_K f_k(x_{ik}) \right), \quad (2)$$

where each segment is of area a_i , and n_i follows some count distribution such as quasi-Poisson, Tweedie, or negative binomial. The f_k are smooth functions, represented by a basis expansion ($f_k(x) = \sum_j \beta_j b_j(x)$, for some basis functions b_j); β_0 is an intercept term, included in parameter vector $\boldsymbol{\beta}$; $\boldsymbol{\lambda}$ is a vector of smoothing (hyper)parameters which control the wiggleness of the f_k . We take a Bayesian interpretation of GAMs, in which $\boldsymbol{\lambda}$ controls the variance of a multivariate improper Gaussian prior (Wood, 2017):

$$\boldsymbol{\beta} \sim N \left(\mathbf{0}, \phi \left(\sum_k \lambda_k \mathbf{S}_k \right)^{-} \right),$$

with scale parameter ϕ , smoothing parameters λ_k and penalty matrices \mathbf{S}_k ($^-$ indicates pseudoinverse). This leads to a quadratic penalty on beta during fitting. We estimate $\boldsymbol{\lambda}$ itself via REML (Wood, 2011), an empirical Bayes procedure. Fully Bayesian approaches, placing hyperpriors on $\boldsymbol{\lambda}$ are also possible.

We are interested in the uncertainty of a predicted abundance estimate, \hat{N} . We assume below that we have created some prediction grid with all density covariates available for each cell in the grid. Abundance is predicted for each cell, and summed for an overall

abundance, \hat{N} , over some region of interest which may not be the entire surveyed area. Although $p(\hat{\boldsymbol{\theta}})$ does not appear explicitly in the prediction, which is

$$\hat{N} = \sum_j a_j \exp \left(\hat{\beta}_0 + \sum_k \hat{f}_k(x_{jk}) \right),$$

the GAM offsets $p(\hat{\boldsymbol{\theta}})$ clearly do affect $\hat{\beta}$, so it is important to account somehow for detection probability uncertainty. (2) assumes the offset is fixed, so extra steps are required.

3 Variance propagation for Density Surface Models

Let $p(\boldsymbol{\theta}_0, z_i)$ be the true probability of detection in segment i and for now omit g , therefore assuming that there are no individual-level covariates (e.g., that group size is always 1) for now (see Section 5). If $\boldsymbol{\theta}_0$ is the true (unknown) value of $\boldsymbol{\theta}$, and $\hat{\boldsymbol{\theta}}$ is its MLE, we use the shorthand $p_i = p(\boldsymbol{\theta}_0, z_i)$ and $\hat{p}_i = p(\hat{\boldsymbol{\theta}}, z_i)$ when the dependence is clear. The expected number of encounters in segment i is $a_i p_i \rho_i$ where ρ_i is the underlying density, given by the exponential term in 2.

Given p_i , we can re-write (2) on the log link scale as:

$$\log \mathbb{E}[n_i | \boldsymbol{\beta}, \boldsymbol{\lambda}, p_i] = \eta_i = \log a_i p_i + X_i \boldsymbol{\beta}. \quad (3)$$

X_i is the (known) i^{th} row of the design matrix, i.e., the values of the basis functions in segment i , so $\log \rho_i = \sum_k f_k(x_{ik}) = X_i \boldsymbol{\beta}$ and $\log a_i p_i$ is an offset. The complication is that we only have an estimate of p_i . To tackle this, we first rewrite the linear predictor η_i as

$$\eta_i = \log a_i + \log \hat{p}_i + \log p_i - \log \hat{p}_i + X_i \boldsymbol{\beta}$$

and then take a Taylor series expansion of $\log \hat{p}_i \equiv \log p(\hat{\boldsymbol{\theta}}, z_i)$ about $\boldsymbol{\theta} = \boldsymbol{\theta}_0$:

$$\log p(\hat{\boldsymbol{\theta}}, z_i) = \log p(\boldsymbol{\theta}_0, z_i) + (\hat{\boldsymbol{\theta}} - \boldsymbol{\theta}_0)^\top \cdot \left[\frac{d \log p(\boldsymbol{\theta}, z_i)}{d \boldsymbol{\theta}} \Big|_{\boldsymbol{\theta}=\boldsymbol{\theta}_0} \right] + O(\hat{\boldsymbol{\theta}} - \boldsymbol{\theta}_0)^2. \quad (4)$$

By defining the vectors $\boldsymbol{\delta} \triangleq \hat{\boldsymbol{\theta}} - \boldsymbol{\theta}_0$ and $\boldsymbol{\kappa}_i \triangleq \frac{d \log p(\boldsymbol{\theta}, z_i)}{d \boldsymbol{\theta}} \Big|_{\boldsymbol{\theta}=\boldsymbol{\theta}_0}$, we can rewrite (3) as

$$\log \mathbb{E}[n_i | \boldsymbol{\beta}, \boldsymbol{\lambda}, \hat{p}_i] = \log a_i \hat{p}_i + X_i \boldsymbol{\beta} + \boldsymbol{\kappa}_i \boldsymbol{\delta} + O(\boldsymbol{\delta}^2). \quad (5)$$

In Supplementary Materials C, we show that the approximations in our approach do not affect the asymptotic order of accuracy. Specifically, the Laplace approximation that underlies REML estimation is accurate to $O(n^{-1})$ and our approximations are of the same order (see Supplementary Materials C for the meaning of n).

We have approximately that $\boldsymbol{\theta}_0 | \mathbf{y} \sim N(\hat{\boldsymbol{\theta}}, \mathbf{V}_\theta) \implies \boldsymbol{\delta} \sim N(\mathbf{0}, \mathbf{V}_\theta)$, where the covariance matrix \mathbf{V}_θ is calculated as the negative inverse Hessian of (1). In other words, the ‘‘posterior distribution’’ of $\boldsymbol{\theta}$ from fitting the detection function now becomes a prior distribution for ρ . To first order, $\boldsymbol{\delta}$ then plays the same structural role in (5) as the basis coefficients $\boldsymbol{\beta}$. The design matrix for $\boldsymbol{\delta}$ ($\boldsymbol{\kappa}$ in (5)) is obtained by differentiating the log-detection probabilities, with respect to $\boldsymbol{\theta}$ at $\hat{\boldsymbol{\theta}}$. Simple 3-point numerical differentiation is

perfectly adequate for calculation of the derivatives. \mathbf{V}_θ should be readily available from detection function fitting (via the Hessian) regardless of the complexity of the model.

This method can be applied automatically to almost any distance sampling setup provided one can calculate detection probabilities, find their derivatives, and obtain a Hessian for the likelihood. Simultaneous estimates β and δ can be obtained from standard GAM fitting software. Posterior inferences about β (therefore ρ and abundance) automatically propagate the uncertainty from fitting the detection function.

The only technical difference from fitting a standard GAM, is that λ is usually unknown and has to be estimated (i.e., the prior on β has known covariance, but unknown scale), whereas the prior on δ is completely determined from the detection function fitting (i.e., in effect $\lambda_\delta = 1/\phi$, where ϕ is the scale parameter). This setup cannot be specified directly in the R package `mgcv` because of implementation details (at least up to version 1.8; it may be possible within other GAM implementations), unless ϕ is fixed rather than estimated. This is fine for Poisson or negative binomial response, but in our experience, better fits can often be obtained using a Tweedie response distribution, for which ϕ must be estimated. In order to implement (5) for a general response distribution using `mgcv`, we therefore use a one-dimensional search over ϕ to maximize the marginal REML. At each iteration, given the working value ϕ^* , we re-fit the GAM fixing $\phi = \phi^*$ and $\lambda_\delta = 1/\phi^*$. Speed can be improved by re-using some of the setup computations (design matrices, etc) at each iteration.

Diagnostics. If the detection function fits properly and the spatial model has adequate flexibility, then the second-stage model should not lead to much change in the detection function parameters, so that $\hat{\delta}$ should be “close” to 0. Nevertheless, there is scope for interaction if the detection function includes covariates that also vary systematically over space. For example, if weather is systematically worse in some parts of the survey region, then both β and θ will contribute to the expected pattern of sightings, and the two sets of parameters are partially confounded. (That is of course also true for all-in-one models, as well for our two-stage model.)

There are several diagnostics that we have found useful for checking consistency between the two parts of the model. The first is to compare the inferred spatial distribution and abundance from fitting (3) with the “naïve” estimates where detection uncertainty is ignored and the offset $a_i \hat{p}_i$ is treated as exact, ensuring that there are not large differences in the estimated spatial distribution. The second is to check whether the detection probabilities (by covariate level) would be substantially changed by fitting the spatial model; in other words, whether $\hat{\delta}$ is close enough to zero given its prior distribution, or, perhaps more usefully, whether the overall detectability by covariate level has changed. Since the fitted spatial model still includes the information from the first stage, any shift of more than about 1 standard deviations (based on the covariance from the detection function stage) might merit investigation. Third, as a general diagnostic tool for density surface models, we have found it useful to compare total observed and expected numbers of sightings, grouped by detection covariates (e.g., Beaufort). This can be helpful in diagnosing detection function problems, e.g., failure of assumed certain detectability at zero distance under poor weather conditions, as well as failures of the spatial model (e.g., an abrupt change in density). In addition one could also use standard detection function model checking (e.g., quantile-quantile plots) with the adjusted parameters, $\hat{\theta} + \hat{\delta}$.

Calculating $\text{Var}(\hat{N})$. Once detection function uncertainty has been propagated, we only need to deal with uncertainty in the GAM, which now has an updated covariance matrix. We therefore can rely on two commonly-used methods to obtain the variance of

model outputs like abundance, \hat{N} .

1. Delta method: We can calculate:

$$\text{Var}(\hat{N}) = \left(\mathbf{a}_p \frac{\partial \exp \mathbf{X}_p \boldsymbol{\beta}}{\partial \boldsymbol{\beta}} \bigg|_{\boldsymbol{\beta}=\hat{\boldsymbol{\beta}}} \right) \mathbf{V}_{\hat{\boldsymbol{\beta}}} \left(\mathbf{a}_p \frac{\partial \exp \mathbf{X}_p \boldsymbol{\beta}}{\partial \boldsymbol{\beta}} \bigg|_{\boldsymbol{\beta}=\hat{\boldsymbol{\beta}}} \right)^\top, \quad (6)$$

(the delta method) where $\mathbf{V}_{\hat{\boldsymbol{\beta}}}$ is the covariance matrix for the GAM coefficients Wood (2017, Sections 5.8 & 6.9.3). We form the prediction matrix, \mathbf{X}_p , which maps model coefficients to values of the linear predictor for the prediction data, so $\hat{\boldsymbol{\eta}}_p = \mathbf{X}_p \hat{\boldsymbol{\beta}}$ (Wood, 2017, Section 6.10). Derivatives are evaluated at the estimated values of the model parameters.

2. Posterior simulation: The posterior for $\boldsymbol{\beta}$ given data \mathbf{y} and smoothing parameters $\boldsymbol{\lambda}$, are approximately distributed as $\boldsymbol{\beta}|\mathbf{y}, \boldsymbol{\lambda} \sim N(\hat{\boldsymbol{\beta}}, \mathbf{V}_{\hat{\boldsymbol{\beta}}})$. The following algorithm then can be used:

1. For $b = 1, \dots, B$:
 - (a) Simulate from $N(\hat{\boldsymbol{\beta}}, \mathbf{V}_{\hat{\boldsymbol{\beta}}})$, to obtain $\hat{\boldsymbol{\beta}}_b$.
 - (b) Calculate predicted abundance, $\hat{N}_b = \mathbf{a}_p \exp(\mathbf{X}_p \hat{\boldsymbol{\beta}}_b)$ (where \mathbf{a}_p is a row vector of areas for the prediction cells).
2. Calculate the empirical variance or percentiles of the \hat{N}_b s.

In practice B in the order of 1000s appears to work well, though there may be some issues when the approximation breaks down. In these cases we recommend the use of importance sampling (either using importance weights to calculate weighted summaries or using a second resampling of the \hat{N}_b s) or a Metropolis-Hastings sampler (as implemented in `mgcv::gam.mh`). Further examples are given in Supplementary Materials.

Software. The procedure given in this section is implemented in the R package `dsm`, available on CRAN. The `dsm_varprop` function in the package allows the user to provide a fitted DSM and a prediction grid. Using the delta method it will then calculate an uncertainty estimate for the estimated abundance for that prediction grid. The function also returns the refitted GAM so one can extract the full covariance matrix and perform posterior simulation if required. Diagnostics for $\hat{\boldsymbol{\delta}}$ are calculated by a `summary` method for the returned object.

4 Previous methods for estimating uncertainty in Density Surface Models

Several approaches have previously been suggested to combine detection function and spatial model predicted abundance uncertainties; we review them briefly here. We need to estimate the following:

$$\begin{aligned} \text{Var}_P(\log N) &= \mathbb{E}_P[\text{Var}(\log N|P)] + \text{Var}_P[\mathbb{E}(\log N|P)] \\ &\approx \text{Var}(\log N|\{\hat{p}_i; i = 1, \dots, n\}) + \text{Var}_P[\log \hat{N}(\{\hat{p}_i; i = 1, \dots, n\})], \end{aligned}$$

where P here is a random variable for the (uncertain) probability of detection and the subscripts indicate the expectation/variance taken over that variable. $\hat{N}(\{\hat{p}_i; i = 1, \dots, n\})$ is the estimated abundance as a function of estimated detection probabilities. The first

part of this can be derived from GAM theory as shown in the previous section; the second is more tricky.

Assuming independence. When \hat{p}_i is the same for all observations, then $N(\hat{p}) \propto 1/\hat{p}$, so \hat{N} and \hat{p} are independent. The total variance of the abundance estimate can be calculated by combining the GAM variance estimate with the variance of the probability of detection summing the squared coefficients of variation ($CV(X) = \sqrt{\text{Var}(X)/\bar{X}}$) (Goodman, 1960). Hence

$$\text{Var}_{\text{IND}}(\hat{N}) = \frac{\hat{N}^2}{\text{CV}^2(\hat{N}_{\text{GAM}}) + \text{CV}^2(\hat{p})}.$$

When there are not covariates in the detection function we calculate:

$$\text{Var}(\hat{p}) = \left(\frac{\partial \hat{p}}{\partial \boldsymbol{\theta}} \Big|_{\boldsymbol{\theta}=\hat{\boldsymbol{\theta}}} \right) \mathbf{V}_{\hat{\boldsymbol{\theta}}} \left(\frac{\partial \hat{p}}{\partial \boldsymbol{\theta}} \Big|_{\boldsymbol{\theta}=\hat{\boldsymbol{\theta}}} \right)^{\text{T}}. \quad (7)$$

This is fine when the detection function does not contain any covariates, as there is no covariance then between the effort and density covariates (the procedure outlined in Section 3 does not yield a different answer). In the case where detectability is a function of covariates it is impossible in general to justify the use of the CV decomposition as there are correlations between the spatial distribution and the covariates affect detectability.

The approach taken by Program Distance (Thomas et al., 2010) is to use Horvitz-Thompson-adjusted counts per segment, instead of the observed count, as the response in the GAM. Thus removes the detectability from the right hand side of (2). Variance is then calculated by taking the probability of detection averaged over the observations by first calculating the Horvitz-Thompson estimate of the abundance in the covered area ($\hat{N} = \sum_i g_i/\hat{p}_i$, where g_i is group size of the i^{th} observation and \hat{p}_i is the probability of detecting that group) then using that \hat{N} to calculate the implied average detectability, had the analysis not contained covariates ($\tilde{p} = \tilde{n}/\hat{N}$, where \tilde{n} is the number of observed groups). The numerical derivatives of \tilde{p} with respect to $\boldsymbol{\theta}$ can then be used in (7) to derive a variance for this probability of detection, averaged over the observations.

We do not recommend this approach either. Transforming the response through multiplication by a random variable breaks the mean-variance and independence assumptions of the GAM, so that the computed CV (\hat{N}_{GAM}) is invalid when detection covariates are present. Additionally, there is no coherent way to generalize the formula to small-area predictions — the effort covariates within a small area will not have the same range as those in the larger survey area (e.g., weather conditions will not be homogenous throughout the survey area). Hence, the uncertainty that applies to the overall \tilde{p} is usually not the appropriate uncertainty to apply to a small area where observing conditions may be atypical.

The bootstrap. Bootstraps are sometimes seen as an attractive alternative to deal with all aspects of variance in DSMs. Hedley and Buckland (2004) describe two possible implementations (one parametric, one non-parametric), which are not easy to choose between and which do not necessarily give similar answers. Ignoring computational time issues, the first practical difficulty in setting up a “good” non-parametric bootstrap for a DSM is sampling units, independent of the fitted model.

The second, more substantial, issue is the fundamental statistical problem with combining smoothers with bootstraps. The problem does not seem to be well-known in the statistical ecology literature, so we give an explanation here. The basic problem is that

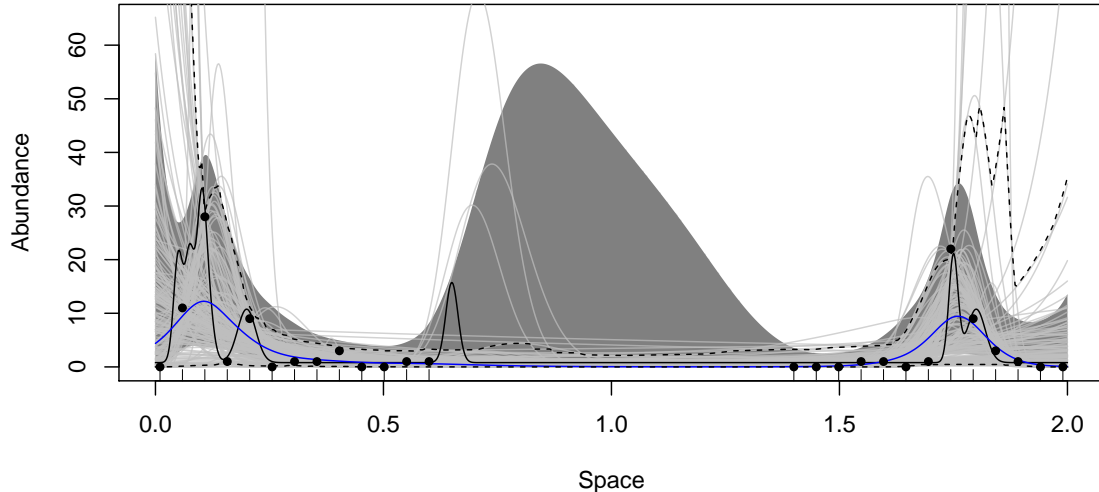


Figure 1: Comparison of bootstrap and analytical uncertainty for a Poisson process. The black line is the true intensity function (on the response scale) and points are observations. Blue line is a smooth of space and light grey wiggly lines are 500 bootstrap predictions, dashed lines are point-wise upper and lower 95% quantiles from the bootstrap, the dark grey band is the analytical GAM confidence band using (6). The bootstrap appears confident that there is nothing in the unsampled area, but the analytical estimate illustrates how little we know.

(most) bootstraps use only the posterior modes of random effects (smooths), thus omitting a key part of the posterior uncertainty. To see this, consider a simple “spatial model” where the region is divided into blocks, each with its own independent random effect, and a bootstrap that generates new data at each original observation/transect, either parametrically or non-parametrically. If one of the blocks is unsampled in the original data, it will be unsampled in every realization too, and the “spatial model” simply sets the point estimate of that random effect to zero in *every* bootstrap realization; hence a bootstrap will ascribe zero uncertainty for the density in that block. The correct inference would of course be for the random effect to retain its prior variance.

This phenomenon has been well-known in statistics since at least Laird and Louis (1987) (see also the discussants), who coined the term “naïve bootstrap” for such procedures that ignore the point estimate shrinkage inevitable in mixed or random effect models (fixed effect models are not susceptible in the same way). They proposed some parametric modifications (“type II” and “type III” bootstraps) that are more effective in the IID and block-structured situations that they consider. However, the underlying theory is complex (Carlin and Gelfand, 1991; Carlin and Louis, 2008) and it is far from clear whether simple yet reliable bootstraps can be devised for complicated multi-stage random effect situations like DSMs. Figure 1 shows a simple unidimensional Poisson process, sampled at either end but not in the middle (rug plot). Bootstrap replicates (shown in light grey, of which there are 500) largely fail to capture our uncertainty in the unsampled middle area. The analytical estimate (dark grey band) illustrates how little we know about the unsampled area.

The above does not imply that simple or indeed complicated bootstraps will *never* give reliable results in DSMs; given plenty of observations and good, uniform coverage, many approaches to inference will give similar and good results. However, it is sometimes

not obvious whether this holds for a specific dataset, nor what to do bootstrap-wise if not. Instead, the (empirical) Bayesian framework of GAMs offers a coherent and general-purpose way to capture uncertainty.

5 A new model for group size

Our variance propagation method so far works if detectability depends only on effort covariates, but not for individual covariates such as group size. Incorporating individual covariates in the detection function is not problematic but it is not obvious how to allow for these different detection probabilities in the GAM. Further, it is not obvious how to combine predictions of different group sizes since average group sizes may vary spatially.

One approach is to use the Horvitz-Thompson-adjusted response described in the previous section, but as mentioned above this does not allow variance propagation. One could fit separate spatial models to subsets of the data for each group size, but it seems inefficient to not share information between subsets of the data. Next, we show instead how to extend our variance-propagation method to deal with group size.

We form M categories of group sizes, denoted $\{g_m; m = 1, \dots, M\}$, where groups within each category have similar detectability, and fit a detection function incorporating these group size categories. We then fit a GAM to an M -fold replicate of the dataset, with the response in the m^{th} replicate of the i^{th} segment being n_{im} , the number of groups in category m that were seen in that segment. (The total number of observations is unchanged; each observation is allocated to just one of the “replicates”.) Group size category (as a factor) is included as an explanatory variable, and smooths are modified to allow similar variations in density of groups with different sizes. There are no extra assumptions in this formulation from the model in Section 3, except to assume that the numbers of groups of different size categories in a given segment are independent, given the underlying density (which is allowed to vary with group size).

Factor-smooth interactions. We extend (2) to include multiple smooths of space which correspond to different categorizations of group size, so our model is:

$$\mathbb{E} \left[n_{i,g_m} \mid \beta, \lambda, p(\hat{\theta}; z_i, g_m) \right] = a_i p(\hat{\theta}; z_i, g_m) \exp \left(\beta_0 + f_{x_1, g_m}(x_{i1}) + \sum_{k=2}^K f_k(x_{ik}) \right), \quad (8)$$

for $m = 1, \dots, M$ where n_{i,g_m} is the number of observed groups in group class g_m in segment i and f_{x_1, g_m} is the spatial smooth (where x_1 is a spatial coordinate) for group size class g_m . Smoothers like f_{x_1, g_m} are referred to as *factor-smooth interactions* (Wood, 2017; Pedersen et al., 2019). f_k are any other smooths (of covariates x_k , for $k > 1$). For clarity we make the dependence on group size class explicit: $p(\hat{\theta}; z_i, g_m)$, i.e., the probability of detection given segment-level detection covariates z_i and group size g_m .

There are a number of different possible forms for f_{x_1, g_m} . These vary in two main ways: (1) do levels share a smoothing parameter, or have separate ones? (2) do smooths tend toward a “global” smooth that dictates a general spatial effect? Here we adopt the “**fs**” basis in `mgcv` which can be thought of as a smooth version of a random slopes model: smooths are generated for each factor level with smooths defined as deviations from a reference level, with all smooths sharing the same smoothing parameter. This is appealing as we might expect that the spatial smooths for each group size are similar but there might be some process that generates larger groups in certain places (e.g., large

prey aggregations attracting large groups of animals). This approach is easily extended to other density covariates (e.g., x_1 could be bathymetry or vegetation cover).

Abundance and uncertainty estimation with group size smooths. Abundance is estimated by summing over the predictions for each group size category (\hat{N}_m) and weighting them by the corresponding mean group size (\bar{g}_m): $\hat{N} = \sum_{m=1}^M \bar{g}_m \hat{N}_m$. We can find $\text{Var}(\hat{N}|\bar{G})$ (where \bar{G} is the mean group size) from the variance propagation procedure above, but we need $\text{Var}(\hat{N})$, which we can obtain from the Law of Total Variance:

$$\begin{aligned} \text{Var}(\hat{N}) &= \mathbb{E}_{\bar{G}}[\text{Var}(\hat{N}|\bar{G})] + \text{Var}[\mathbb{E}_{\bar{G}}(\hat{N}|\bar{G})] \\ &= \text{Var}(\hat{N}|\bar{G}) + \sum_{m=1}^M \text{Var}(\bar{G}_m) \hat{N}_m^2, \end{aligned} \tag{9}$$

where $\text{Var}(\bar{G}_m)$ reflects the uncertainty about mean group size within a category, to be estimated empirically from all the observed groups in that category. The effect of $\text{Var}(\bar{G}_m)$ on $\text{Var}(N)$ should be small (because categories are narrow, and mean must lie within category), and also should not vary much spatially, so no further spatial adjustment to that variance component is required.

6 Examples

Island Scrub-Jays. We first apply our variance propagation method in a simple situation where there is covariance between the abundance and detection processes, that is the case of a spatially-varying detection covariate. Island Scrub-Jays (*Aphelocoma insularis*) are endemic to Santa Cruz Island, California. Jays primarily reside in areas of chaparral and forest, though the density of this foliage also affects detectability. Sillett et al. (2012) model the distribution Island Scrub-Jays from 307 point transects surveyed in fall 2008 and spring 2009. Distances were binned into three intervals due to responsive movement ($[0m - 100m]$, $(100m - 200m]$, $(200m - 300m]$). Proportion chaparral (**chap**) and proportion forest (**forest**) were available as covariates, as was elevation (**elev**). Sillett et al. fitted a hierarchical model assuming a negative binomial distribution for abundance and a multinomial detection process using a half-normal detection function. Their best models (by AIC) were: fall 2008 abundance modelled as $\beta_0 + \beta_1 \text{chap}^2 + \beta_2 \text{chap} + \beta_3 \text{elev}$, with detectability as a function of **chap**; spring 2009 abundance modelled as $\beta_0 + \beta_1 \text{chap}^2 + \beta_2 \text{chap} + \beta_3 \text{elev}^2 + \beta_4 \text{elev}$, detectability as a function of **forest**.

We replicated the analysis of Sillett et al. using our two-stage variance propagation approach to show that our method can be used in such a situation. In summary, final coefficient estimates were very close to those in the original paper, abundance estimates with associated 95% CIs were very similar for both seasons: Fall 2008 DSM $\hat{N} = 2272$ (1625–3175), Sillett et al. $\hat{N} = 2267$ (1613–3007) and Spring 2009 DSM $\hat{N} = 1684$ (1263–2246), Sillett et al. $\hat{N} = 1705$ (1212–2369); Supplementary Material A gives the comparison in full. For the spring model, the value of the **forest** coefficient in the detection function changed effect size from -0.18 (SE=0.06) to -0.083 (SE=0.062) after propagation (indicating no issue with our $\hat{\delta}$ diagnostic). By giving the GAM the flexibility to slightly adjust the detection function parameters via $\hat{\delta}$ (as opposed to treating the estimated detection probabilities as certain), the CV of the abundance estimate is actually improved in this case, from 18.4% to 14.8%.

The jay data presents a particularly interesting case as the covariates in the GAM

are fixed effects, there is therefore no “cost” (in terms of the penalized likelihood) to changing the GAM coefficients. We see minimal changes in the parameters of the fall model (Supplementary Material A, Table 1), as these are already well modelled (no doubt due to the good coverage of the data): the detection function includes `chap` and the GAM includes `chap` and `chap2`, so any adjustment via $\hat{\delta}$ is a 3rd order effect. The spring model has different covariates in each model component, making the correction necessary.

The survey design had extremely good coverage over Santa Cruz Island. We decided to see what the effect of “unbalancing” the design would be to test the robustness of our model. We randomly subsampled the fall data to contain only 100 sites, then removed those where chaparral cover was greater than the mean chaparral proportion (over all points). Our subsample was left with 16 detections at 65 points. Fitting the fall DSM to the reduced data yields $\hat{N} = 26,434$ (95% CI 209-3,349,000; CV=2,100%). Post-variance propagation, we obtain $\hat{N} = 2,831$ (95% CI 39-206,000; CV=1,100%), both detection function and GAM coefficients having changed (see Supplementary Material A, Table 3). While we would expect a high variance for such a small and unbalanced dataset (and indeed we obtain this), our procedure tames the model to an extent, giving a more realistic estimate of abundance. Once information about both model components is allowed to inform the parameter estimation simultaneously, the coefficients are corrected.

Island Scrub-Jays Simulation. To assess performance of our variance propagation method with the delta method and a one stage fully Bayesian approach we conducted a simulation using the Island Scrub-Jay data as a starting point. We kept spatial coverage constant throughout the simulation settings but varied the detectability and therefore the number of observations available for the detection function component of the model. Full details of the simulation setup are given in Supplementary Material B. Here we note that our variance propagation method performed well in terms of bias in the abundance estimate and its corresponding variance estimate compared to the fully Bayesian model, even when sample size decreased (Supplementary Material B, Figure 2).

Harbour porpoise. To illustrate our new group size model, we re-analyse an aerial line transect survey of harbour porpoise in Irish Sea, coastal Irish waters and Western coastal Scotland, where we see spatial variation in observed group size of 1 to 5 animals (typical for harbour porpoise; e.g., Siebert et al., 2006; points in Figure 2). During SCANS-II aerial surveys, two observers recorded cetacean detections (along with sighting conditions) from bubble windows on both sides of a plane flying at 183m. Complete survey details and a comprehensive analysis is given in Hammond et al. (2013). For simplicity we assume certain detection on the trackline, no errors in group size estimation (less likely with aerial than in shipboard surveys for harbour porpoise; Phil Hammond, Debi Palka, *pers. comm.*, November 2017), and negligible island/coastline effects in the spatial model.

To fit our DSM, three group size bins were formed: size 1 (131 observations), 2 (35 observations) and 3-5 (14 observations). A hazard-rate detection function was fitted to the observed distances (truncated at 300m) with the group size bin (g_m , $m = 1, \dots, 3$) and Beaufort (B_i , binned as 0-1, 2 and 3-5) as factor covariates. Detectability for each segment i per group size factor was then estimated from the detection function: $p(\hat{\theta}; B_i, g_m)$. Following (8) we fitted the DSM:

$$\mathbb{E} \left[n_{i,g_m} | \beta, \lambda, p(\hat{\theta}; B_i, g_m) \right] = a_i p(\hat{\theta}; B_i, g_m) \exp(\beta_0 + f_{E,N,g_m}(E_i, N_i)),$$

where in segment i of area a_i the observed number of groups in size category g_m was denoted n_{i,g_m} . It was assumed the response was Tweedie-distributed where the power

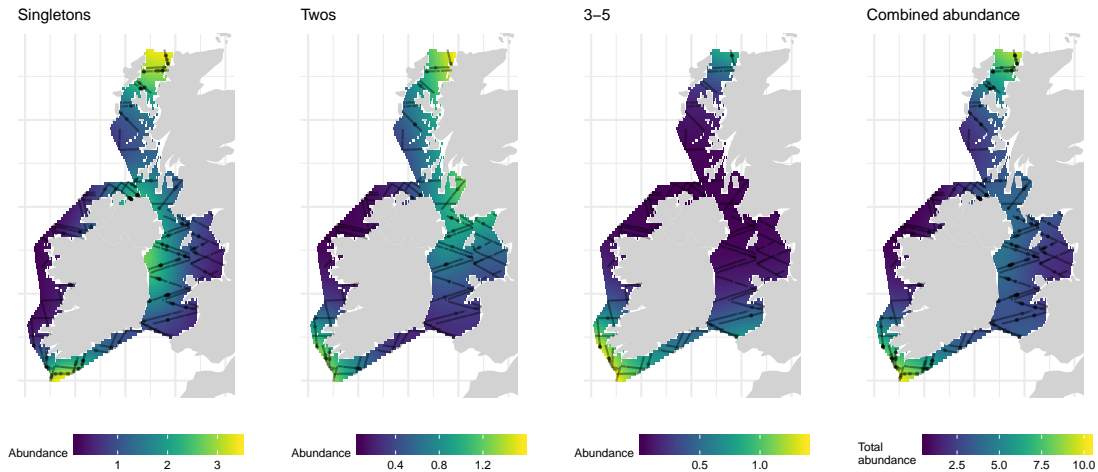


Figure 2: Predicted density surfaces from the new group size model for harbour porpoise. First three plots are density maps for the given group size (i.e., group abundance multiplied by mean group size), right plot shows the combined map, summing the previous three plots per prediction cell. We can see that distribution is roughly similar in all three group size categories though with almost no larger groups in the North, far more animals occurring as singletons than in larger groups.

parameter was constrained to be greater than 1.2 to avoid numerical issues. Each f_{E,N,g_m} was a smooth of space (projected Easting/Northing; E_i, N_i) for group category g_m and had a maximum basis size of 20 (total maximum basis size for f_{E,N,g_m} was therefore 60).

The fitted model had a total effective degrees of freedom of 20.47 for f_{E,N,g_m} . GAM checking showed reasonable fit to the data. Table 1 shows observed vs expected counts by Beaufort — there is some misfit at the highest state, perhaps because detection probability at zero distance changes with Beaufort level (from Hammond et al.: 0.45 for Beaufort 0-1 and 0.31 in Beaufort 2-3). Plots of the per-group size bin predictions and the combined prediction are given in Figure 2, which show some consistent patterns between group size classes (“hotspot” off Southern Ireland) and some differences (varying distribution in the Irish Sea and Western Scotland), this kind of insight is not possible using a single smooth for all observations and may prove useful in cases where there are occasional very large group sizes (e.g., oceanic dolphins). Using (7), the CV of abundance was estimated to be 2.36%, when our new variance propagation method was used the CV was estimated as 9.65%. The assumption of independence (via (7)) underestimates uncertainty in the case where group size (and detectability) vary in space. Only a small piece of code implementing (9) was required in addition to the `dsm_varprop` function (included in Supplementary Material A), we then gain the ability to make inferences about group size spatial distribution (traditionally requiring two separate models, one for encounter rate, one for group size; e.g., Becker et al., 2014), as well as improve uncertainty estimation via variance propagation.

7 Discussion

Combining the uncertainty from detection functions with that from spatial models has been a challenging problem for point and line transect analysis, requiring either compli-

Table 1: Observed versus expected counts from the harbour porpoise DSM (post-variance propagation) at levels of Beaufort used in the detection function.

	0-1	2	3-5
Observed	98.00	36.00	30.00
Expected	96.59	35.13	35.69

cated bespoke software that combines two model components, or ad hoc approaches that lack statistical justification. In this paper, we have demonstrated a simple, flexible, and statistically sound method that can (i) propagate uncertainty from detectability models to the spatial models for a particular class of detection function (i.e., those without individual-level covariates) and (ii) include group size as a covariate in the detection function while still being able to propagate uncertainty and address spatial variation in group size. Our methods are implemented in the `dsm` package for R but can be implemented in any standard GAM fitting software.

It is straightforward to apply our factor-smooth approach group size more generally to individual-level covariates which affect detectability and vary in space, but do not directly affect abundance, such as observable behaviour. For example, feeding groups might be more (or less) conspicuous than resting groups, and the proportion feeding/resting may vary across the surveyed region. Unless detectability is included in the analysis, biased abundance estimates could result, especially when survey coverage is non-uniform; and there has been no simple way until now to include such effects in the spatial model. A major advantage of our approach over simple (or complex) stratification schemes is that we are now sharing information between the levels of our categorized variable. This makes the results less sensitive to over-specifying the number of categories, as the model will shrink back towards the simpler model in the absence of strongly informative data. We also note that the factor-smooth approach could be applied to all smooth terms in the GAM, allowing for a very flexible model. This would be appropriate only if it was reasonable that all smooths vary according to the detectability covariate (e.g., feeding behaviour in our harbour porpoise example might depend on both space and depth).

We have assumed that all variables are measured without much error. Measurement error for individual-level covariates such as group size can be a serious problem in distance sampling (Hodgson et al., 2017)—distance between observer and group can affect not just detectability, but also the extent of group size error. If group size varies spatially, it is hard to see how to separate the spatial modelling stage from the distance sampling stage. A full discussion is beyond the scope of this paper, but we suspect that specially-designed observation protocols and bespoke analyses may be the only way to tackle such thorny cases.

All-in-one fitting of both detection and spatial models is also possible (e.g., Johnson et al., 2009; Sillett et al., 2012; Yuan et al., 2017). If models are specified correctly, then the all-in-one approach could in theory be slightly more efficient, but only insofar as it takes account of third-order changes in the detection function likelihood (since our approach uses a quadratic approximation). That seems unlikely to make much difference in general—and as is the case for the Island Scrub-jay example. Our own preference is therefore to use the two-stage approach, mainly because in our experience the careful fitting of detection functions is a complicated business which can require substantial model exploration and as few as possible “distractions” (such as simultaneously worrying about the spatial model). The two-stage process allows any form of detection function

to be used, without having to make deep modifications to software. In summary, if one *knew* one had the correct model to begin with, one-stage fitting would be slightly more efficient, but this is never the case in practice.

It is valuable to check for any tension or confounding between the detection function and density surface parts of the model, which can occur if there are large-scale variations in sighting conditions across the survey region, and which is readily diagnosed in a two-stage model. Although this does not appear to lead to problems in the datasets we have analysed with the software described in this paper, we have come across it in other variants of line transect-based spatial models with different datasets. It may not be so easy to detect partial confounding when using all-in-one frameworks.

Finally, we note that the approach outlined here (of using a first-stage estimate as a prior for a second-estimate, and propagating variance appropriately) is quite general and is comparable to standard sequential Bayesian approaches to so-called “integrated data models”. The first-stage model need not be a detection function but instead could be from another GAM (or other latent Gaussian model). Again, this allows us to ensure that first-stage models are correct before moving to more complex modelling. Modelling need not only be two-stage and could extend to multi-stage models (Hooten et al., 2019).

Acknowledgements

The authors thank Natalie Kelly, Jason Roberts, Eric Rexstad, Phil Hammond, Steve Buckland and Len Thomas for useful discussions, Devin Johnson for the suggestion of this as a general statistical method, and Simon Wood for continued development of `mgcv` and GAM theory. The manuscript was greatly improved by comments from the editor and two anonymous reviewers. Data from the SCANS-II project was supported by the EU LIFE Nature programme (project LIFE04NAT/GB/000245) and governments of range states: Belgium, Denmark, France, Germany, Ireland, Netherlands, Norway, Poland, Portugal, Spain, Sweden and UK. This work was funded by OPNAV N45 and the SURTASS LFA Settlement Agreement, and being managed by the U.S. Navy’s Living Marine Resources program under Contract No. N39430-17-C-1982, US Navy, Chief of Naval Operations (Code N45), grant number N00244-10-1-0057 and the International Whaling Commission.

References

- E. A. Becker, K. A. Forney, D. G. Foley, R. C. Smith, T. J. Moore, and J. Barlow. Predicting seasonal density patterns of California cetaceans based on habitat models. *Endangered Species Research*, 23(1):1–22, Jan. 2014.
- D. L. Borchers, W. Zucchini, and R. M. Fewster. Mark-Recapture Models for Line Transect Surveys. *Biometrics*, 54(4):1207, 1998.
- S. T. Buckland, D. R. Anderson, K. P. Burnham, D. L. Borchers, and L. Thomas. *Introduction to Distance Sampling*. Estimating Abundance of Biological Populations. Oxford University Press, Oxford, UK, 2001.
- B. P. Carlin and A. E. Gelfand. A sample reuse method for accurate parametric empirical Bayes confidence intervals. *Journal of the Royal Statistical Society: Series B*, 1991.

- B. P. Carlin and T. A. Louis. *Bayesian Methods for Data Analysis, Third Edition*. CRC Press, 2008.
- L. A. Goodman. On the Exact Variance of Products. *Journal of the American Statistical Association*, 55(292):708, 1960.
- P. S. Hammond, K. Macleod, P. Berggren, D. L. Borchers, L. Burt, A. Cañadas, et al. Cetacean abundance and distribution in European Atlantic shelf waters to inform conservation and management. *Biological Conservation*, 164(C):107–122, 2013.
- S. L. Hedley and S. T. Buckland. Spatial models for line transect sampling. *Journal of Agricultural, Biological, and Environmental Statistics*, 9(2):181–199, 2004.
- A. Hodgson, D. Peel, and N. Kelly. Unmanned aerial vehicles for surveying marine fauna: assessing detection probability. *Ecological applications : a publication of the Ecological Society of America*, 27(4):1253–1267, 2017.
- M. B. Hooten, D. S. Johnson, and B. M. Brost. Making recursive Bayesian inference accessible. *The American Statistician*, 2019.
- D. S. Johnson, J. L. Laake, and J. M. Ver Hoef. A Model-Based Approach for Making Ecological Inference from Distance Sampling Data. *Biometrics*, 66(1):310–318, 2009.
- N. M. Laird and T. A. Louis. Empirical Bayes Confidence Intervals Based on Bootstrap Samples. *Journal of the American Statistical Association*, 82(399):739–750, 1987.
- F. F. C. Marques and S. T. Buckland. Incorporating covariates into standard line transect analyses. *Biometrics*, 59(4):924–935, 2003.
- T. A. Marques, S. T. Buckland, R. Bispo, and B. Howland. Accounting for animal density gradients using independent information in distance sampling surveys. *Statistical Methods & Applications*, 22(1):67–80, 2012.
- D. L. Miller, M. L. Burt, E. A. Rexstad, and L. Thomas. Spatial models for distance sampling data: recent developments and future directions. *Methods in Ecology and Evolution*, 4(11):1001–1010, Aug. 2013.
- E. J. Pedersen, D. L. Miller, G. L. Simpson, and N. Ross. Hierarchical generalized additive models: an introduction with mgcv. *PeerJ*, page e6876, 2019.
- U. Siebert, A. Gilles, K. Lucke, M. Ludwig, H. Benke, K.-H. Kock, and M. Scheidat. A decade of harbour porpoise occurrence in german waters—analyses of aerial surveys, incidental sightings and strandings. *Journal of Sea Research*, 56(1):65–80, 2006.
- T. S. Sillett, R. B. Chandler, J. A. Royle, M. Kéry, and S. A. Morrison. Hierarchical distance-sampling models to estimate population size and habitat-specific abundance of an island endemic. *Ecological Applications*, 22(7):1997–2006, 2012.
- H. J. Skaug and T. Schweder. Hazard models for line transect surveys with independent observers. *Biometrics*, 55(1):29–36, 1999.
- L. Thomas, S. T. Buckland, E. A. Rexstad, J. L. Laake, S. Strindberg, S. L. Hedley, et al. Distance software: design and analysis of distance sampling surveys for estimating population size. *Journal of Applied Ecology*, 47(1):5–14, Feb. 2010.

- S. N. Wood. Fast stable restricted maximum likelihood and marginal likelihood estimation of semiparametric generalized linear models. *Journal of the Royal Statistical Society: Series B (Statistical Methodology)*, 73(1):3–36, 2011.
- S. N. Wood. *Generalized Additive Models: An Introduction with R, Second Edition*. Chapman & Hall/CRC Texts in Statistical Science. CRC Press, 2017.
- Y. Yuan, F. E. Bachl, F. Lindgren, D. L. Borchers, I. J. B., S. T. Buckland, et al. Point process models for spatio-temporal distance sampling data from a large-scale survey of blue whales. *The Annals of Applied Statistics*, 11(4):2270–2297, 2017.

Supplementary Material A: Island Scrub-jay analysis

Mark V. Bravington
David L. Miller
Sharon L. Hedley

December 29, 2020

1 Introduction

This analysis is based on data from the paper:

Sillett, T. Scott, Richard B. Chandler, J. Andrew Royle, Marc Kery, and Scott A. Morrison. 'Hierarchical Distance-Sampling Models to Estimate Population Size and Habitat-Specific Abundance of an Island Endemic'. Ecological Applications 22, no. 7 (2012): 1997-2006

Data is available at: https://figshare.com/articles/Supplement_1_R_code_data_and_grid_covariates_used_in_the_analyses_/3517754. Script `get_issj_data.R` converts this to a dsm-compatible format (or use `issj.RData`).

The authors analyse 2 point transect surveys of Island Scrub-jays from Santa Cruz Island, CA. Each survey consists of 307 sample locations (point transects), one occurring in fall 2008 and the other in spring 2009. Distances were binned into 3 intervals. Locations of the points were available, along with vegetation (proportion forest and proportion chaparral) and elevation. They dredged the data (see their table 2), but their two final models were:

Fall 2008 model: abundance was given as $\beta_0 + \beta_1 \text{chaparral}^2 + \beta_2 \text{chaparral} + \beta_3 \text{elevation}$, detectability as a function of `chaparral`.

Spring 2009 model: abundance was given as $\beta_0 + \beta_1 \text{chaparral}^2 + \beta_2 \text{chaparral} + \beta_3 \text{elevation}^2 + \beta_4 \text{elevation}$, detectability as a function of `forest`.

In both cases, abundance was assumed negative binomially distributed and a half-normal detection function was fitted.

2 Analysis

Reproducing the analysis from Sillet et al. First loading the requisite data and R packages.

```
# load data
load("issj.RData")

# load packages
library(Distance)

## Loading required package: mrds
## This is mrds 2.2.4
## Built: R 4.0.2; ; 2020-11-30 17:31:53 UTC; unix
##
## Attaching package: 'Distance'
## The following object is masked from 'package:mrds':
##
##   create.bins

library(dsm)
```

```
## Loading required package: mgcv
## Loading required package: nlme
## This is mgcv 1.8-33. For overview type 'help("mgcv-package")'.
## Loading required package: numDeriv
## This is dsm 2.3.1.9007
## Built: R 4.0.2; ; 2020-10-30 08:32:41 UTC; unix
```

2.1 Fall 2008

Running models:

```
# fit detection function
df_fall <- ds(obs_fall, transect="point", formula=~chaparral)

## Columns "distbegin" and "distend" in data: performing a binned analysis...
## Model contains covariate term(s): no adjustment terms will be included.
## Fitting half-normal key function
## AIC= 330.658
## No survey area information supplied, only estimating detection function.

# fit spatial model
ll_fall <- dsm(count~chaparral +
               I(chaparral^2) +
               elevation,
               observation.data=obs_fall, segment.data=segs, ddf.obj=df_fall,
               transect="point", family=nb())

# check parameter estimates
summary(ll_fall)

##
## Family: Negative Binomial(0.343)
## Link function: log
##
## Formula:
## count ~ chaparral + I(chaparral^2) + elevation + offset(off.set)
##
## Parametric coefficients:
##              Estimate Std. Error z value Pr(>|z|)
## (Intercept)  -11.7170    0.1682 -69.656 < 2e-16 ***
## chaparral     1.4288     0.1906   7.496 6.57e-14 ***
## I(chaparral^2) -0.3789    0.1255  -3.019 0.00254 **
## elevation    -0.2260    0.1478  -1.528 0.12639
## ---
## Signif. codes:  0 '***' 0.001 '**' 0.01 '*' 0.05 '.' 0.1 ' ' 1
##
##
## R-sq.(adj) = 0.026  Deviance explained = 25.9%
## -REML = 270.86  Scale est. = 1          n = 307
```

We can then do the variance propagation via the `dsm_varprop` function and compare to the delta method (implemented in the `dsm.var.gam` function):

```
# varprop
pp_fall <- dsm_varprop(ll_fall, pred)
pp_fall
```

```

## Summary of uncertainty in a density surface model calculated
## by variance propagation.
##
## Probability of detection in fitted model and variance model
##   chaparral Fitted.model Fitted.model.se Refitted.model
## 1 -0.8613374   0.3345638   0.04953141   0.3383015
## 2  0.1733685   0.2350608   0.02187221   0.2361407
## 3  2.0242947   0.1166973   0.01900894   0.1154638
##
## Approximate asymptotic confidence interval:
##   2.5%   Mean   97.5%
## 1625.431 2271.870 3175.400
## (Using log-Normal approximation)
##
## Detection function CV           : 0.0897
##
## Point estimate                   : 2271.87
## Standard error                   : 390.9639
## Coefficient of variation         : 0.1721

# delta method for comparison
vg_fall <- dsm.var.gam(ll_fall, pred, off.set=pred$off.set)
vg_fall

## Summary of uncertainty in a density surface model calculated
## analytically for GAM, with delta method
##
## Approximate asymptotic confidence interval:
##   2.5%   Mean   97.5%
## 1614.289 2270.436 3193.281
## (Using log-Normal approximation)
##
## Point estimate                   : 2270.436
## CV of detection function         : 0.08974614
## CV from GAM                     : 0.1506
## Total standard error            : 398.1164
## Total coefficient of variation   : 0.1753

```

2.2 Spring 2009

Again fitting models:

```

# fit detection function
df_spring <- ds(obs_spring, transect="point", formula=~forest)

## Columns "distbegin" and "distend" in data: performing a binned analysis...
## Model contains covariate term(s): no adjustment terms will be included.
## Fitting half-normal key function
## AIC= 303.83
## No survey area information supplied, only estimating detection function.

# fit spatial model
ll_spring <- dsm(count~chaparral +
                 I(chaparral^2) +
                 elevation +
                 I(elevation^2),

```

```

        observation.data=obs_spring, segment.data=segs, ddf.obj=df_spring,
        transect="point", family=nb())

# check parameter estimates
summary(ll_spring)

##
## Family: Negative Binomial(0.672)
## Link function: log
##
## Formula:
## count ~ chaparral + I(chaparral^2) + elevation + I(elevation^2) +
##   offset(off.set)
##
## Parametric coefficients:
##              Estimate Std. Error z value Pr(>|z|)
## (Intercept)  -11.43571    0.17886  -63.936 < 2e-16 ***
## chaparral     0.68155    0.15642   4.357 1.32e-05 ***
## I(chaparral^2) -0.31515    0.10730  -2.937 0.00331 **
## elevation    -0.08065    0.15006  -0.537 0.59098
## I(elevation^2) -0.33865    0.15125  -2.239 0.02515 *
## ---
## Signif. codes:  0 '***' 0.001 '**' 0.01 '*' 0.05 '.' 0.1 ' ' 1
##
##
## R-sq.(adj) = 0.0727   Deviance explained = 12.3%
## -REML = 276.52   Scale est. = 1           n = 307

```

Compare variance calculations:

```

# varprop
pp_spring <- dsm_varprop(ll_spring, pred, trace=TRUE)
pp_spring

## Summary of uncertainty in a density surface model calculated
## by variance propagation.
##
## Probability of detection in fitted model and variance model
##      forest Fitted.model Fitted.model.se Refitted.model
## 1 -0.4633652    0.2710221    0.02760400    0.2514265
## 2 -0.3424751    0.2604019    0.02555611    0.2468799
## 3  2.5274876    0.0933240    0.03014374    0.1569675
##
## Approximate asymptotic confidence interval:
##      2.5%      Mean      97.5%
## 1262.702 1684.184 2246.355
## (Using log-Normal approximation)
##
## Detection function CV           : 0.142
##
## Point estimate                   : 1684.184
## Standard error                   : 248.8427
## Coefficient of variation         : 0.1478

# delta method for comparison
vg_spring <- dsm.var.gam(ll_spring, pred, off.set=pred$off.set)
vg_spring

```

```

## Summary of uncertainty in a density surface model calculated
## analytically for GAM, with delta method
##
## Approximate asymptotic confidence interval:
##   2.5%      Mean      97.5%
## 1187.849 1697.548 2425.956
## (Using log-Normal approximation)
##
## Point estimate           : 1697.548
## CV of detection function  : 0.1420396
## CV from GAM              : 0.1165
## Total standard error     : 311.8206
## Total coefficient of variation : 0.1837

```

3 Comparing to results in Sillet et al.

Table 1 compares the parameter estimates from Sillet et al. (their Table 3) with the results from using the DSMs described above.

To obtain uncertainty estimates of detection function parameters we require the following function to recompute the Hessian for that model component.

```

# wee function to get a "corrected" detection function
# note this only works for half-normal models
# the function's argument object is the result from dsm_varprop
fix_ddf_vp <- function(object){
  # get the model from the varprop object
  fix_ddf <- object$old_model$ddf
  # get parameters
  which.names <- !(names(coef(object$refit)) %in% names(coef(object$old_model)))
  newpar <- fix_ddf$par + coef(object$refit)[which.names]

  # setup a new fitting call
  fix_call <- fix_ddf$call
  fix_ddf$control$initial <- list()
  fix_ddf$control$initial$scale <- newpar

  # ensure that the model is not fitted!
  # Just want to calculate the Hessian!
  fix_ddf$control$maxiter <- 0
  fix_ddf$control$refits <- 0
  fix_ddf$control$refit <- FALSE
  fix_ddf$control$nofit <- TRUE

  # run the model and return it
  fix_ddf <- eval(fix_call, fix_ddf)
  invisible(fix_ddf)
}

# corrected for fall
vp_ddf_fall <- fix_ddf_vp(pp_fall)

# corrected for spring
vp_ddf_spring <- fix_ddf_vp(pp_spring)

```

Table 2 compares the abundance estimates from from Sillet et al. to the estimates here.

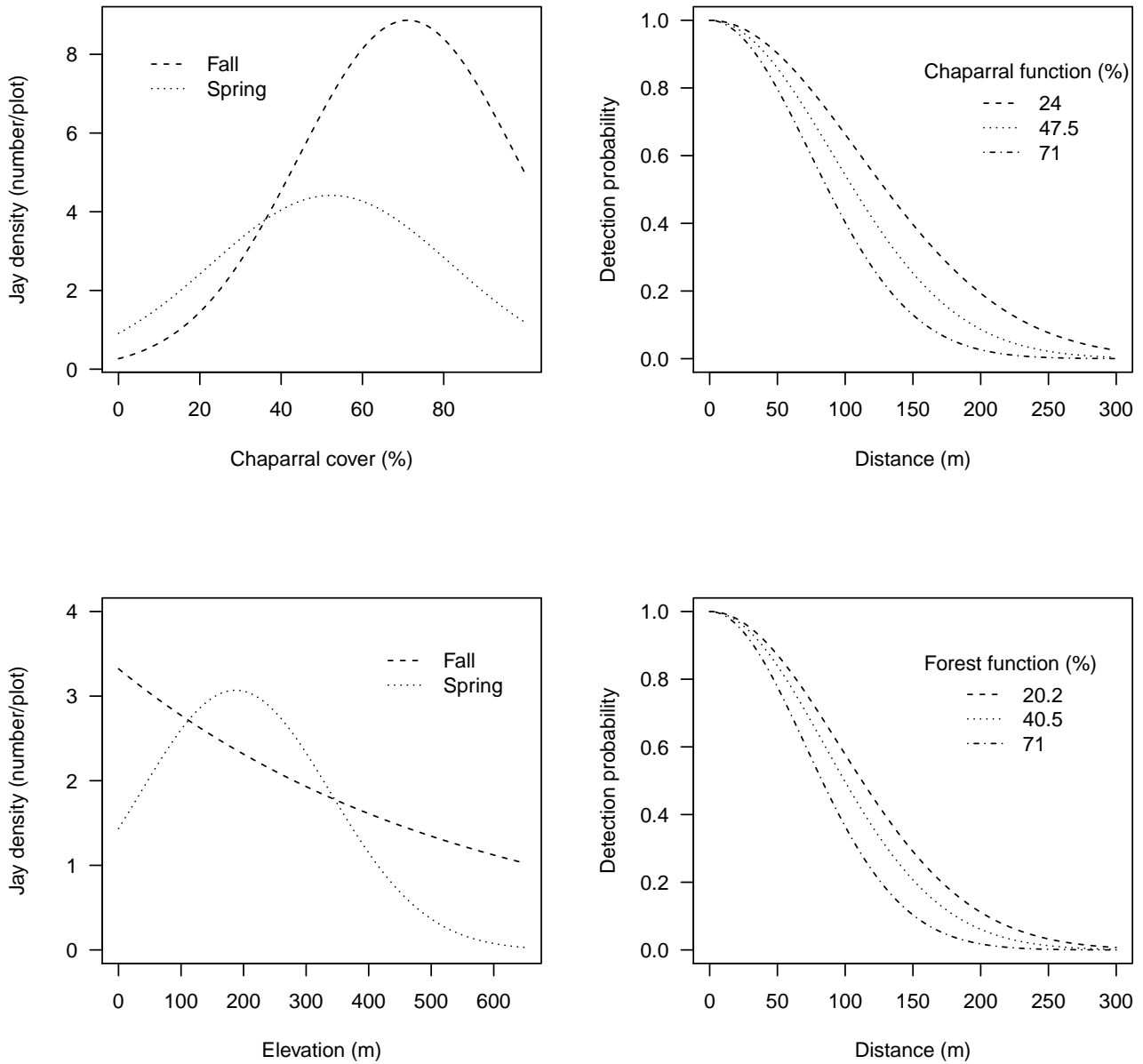


Figure 1: Reproduction of Figure 4 from Sillet et al. using the models specified above. Left side shows abundance per site as a function of the covariates in each time period. Right side shows the detection function at selected covariate levels for fall (top) and spring (bottom). These are indistinguishable from those in the article.

Submodel and coefficient	Fall 2008			Spring 2009		
	Sillet et al.	Pre-varprop	Post-varprop	Sillet et al.	Pre-varprop	Post-varprop
Abundance						
Chaparral	1.43 (0.229)	1.43 (0.191)	1.44 (0.209)	0.67 (0.667)	0.68 (0.156)	0.67 (0.156)
Chaparral ²	-0.38 (0.115)	-0.38 (0.126)	-0.38 (0.126)	-0.29 (-0.291)	-0.32 (0.107)	-0.29 (0.106)
Elevation	-0.23 (0.146)	-0.23 (0.148)	-0.23 (0.148)	-0.11 (-0.107)	-0.08 (0.15)	-0.11 (0.148)
Elevation ²				-0.34 (0.148)	-0.34 (0.151)	-0.34 (0.15)
Dispersion	0.36 (0.0777)	0.34	0.34	0.78 (0.239)	0.71	0.71
Detection						
Intercept	4.68 (0.0658)	4.67 (0.055)	4.68 (0.055)	4.63 (0.540)	4.63 (0.051)	4.64 (0.05)
Chaparral	-0.20 (0.060)	-0.19 (0.052)	-0.2 (0.052)			
Forest				-0.09 (0.043)	-0.18 (0.06)	-0.08 (0.062)

Table 1: Comparison of parameter estimates from Sillet et al. to those using DSM (before and after our variance propagation procedure). Note that `mgcv` (and hence the `dsm` package) does not provide uncertainty around the negative binomial parameter. Abundance intercept parameters are not comparable and therefore omitted (due to differences in how the offset is calculated in each model).

	Fall 2008	Spring 2009
Sillet et al.	2267 (1613–3007)	1705 (1212–2369)
DSM	2272 (1625–3175)	1684 (1263–2246)

Table 2: Comparison of abundance estimates between Sillet et al. and the above analysis.

4 Unbalanced data

Since the coverage of both covariate and geographical space is extremely good, we decided to subsample the data to see what effect that had on our models. We used the fall data only for this experiment and randomly selected 100 points. We then removed points where where chaparral cover was greater than the mean chaparral proportion (with mean calculated over all points).

```
# reproducible subsample
set.seed(1889)

# take 100 sites at random
sub_segs <- segs[sample(1:nrow(segs), 100), ]
# only the observations at those sites are to be included
sub_obs <- obs_fall[obs_fall$Sample.Label %in% sub_segs$Sample.Label, ]

# since the data were z-transformed, mean=0
# so chaparral<=0 gives values at or lower than the mean
sub_segs <- sub_segs[sub_segs$chaparral<=0, ]
sub_obs <- sub_obs[sub_obs$chaparral<=0, ]
```

Having subsampled the data, we can then fit models:

```
# fall detection function on subsampled data
sub_df <- ds(sub_obs, transect="point", formula=~chaparral)

## Columns "distbegin" and "distend" in data: performing a binned analysis...
## Model contains covariate term(s): no adjustment terms will be included.
## Fitting half-normal key function
## AIC= 31.544
## No survey area information supplied, only estimating detection function.

# fall GAM
sub_ll <- dsm(count~chaparral +
```



```

      I(chaparral^2) +
      elevation,
      observation.data=sub_obs, segment.data=sub_segs, ddf.obj=sub_df,
      transect="point", family=nb())

# inspect coefficient estimates
summary(sub_ll)

##
## Family: Negative Binomial(0.222)
## Link function: log
##
## Formula:
## count ~ chaparral + I(chaparral^2) + elevation + offset(off.set)
##
## Parametric coefficients:
##           Estimate Std. Error z value Pr(>|z|)
## (Intercept)  -10.8052    1.6186  -6.676 2.46e-11 ***
## chaparral     3.7674     6.4030   0.588  0.556
## I(chaparral^2) -0.9836     5.1426  -0.191  0.848
## elevation    -0.6331     0.4901  -1.292  0.196
## ---
## Signif. codes:  0 '***' 0.001 '**' 0.01 '*' 0.05 '.' 0.1 ' ' 1
##
##
## R-sq.(adj) = 0.167  Deviance explained = 50.5%
## -REML = 26.603  Scale est. = 1          n = 65

```

Compare variance calculations:

```

# variance propagation:
sub_pp <- dsm_varprop(sub_ll, pred)
sub_pp

## Summary of uncertainty in a density surface model calculated
## by variance propagation.
##
## Probability of detection in fitted model and variance model
##   chaparral Fitted.model Fitted.model.se Refitted.model
## 1 -0.9059225  0.7806223      0.5482305      0.6638134
## 2 -0.3043294  0.2713778      0.1688496      0.2792179
## 3 -0.1975517  0.1967457      0.1929185      0.2233795
##
## Approximate asymptotic confidence interval:
##           2.5%           Mean           97.5%
##           38.84062  2831.42634 206406.98577
## (Using log-Normal approximation)
##
## Detection function CV           : 0.7106
##
## Point estimate                   : 2831.426
## Standard error                   : 30908.15
## Coefficient of variation         : 10.9161

# delta method
sub_vg <- dsm.var.gam(sub_ll, pred, off.set=pred$off.set)
sub_vg

```

	Pre-varprop	Post-varprop
Full data	2270 (1614-3193)	2272 (1625-3175)
Subsample	26434 (209-3348966)	2831 (39-206407)

Table 3: Comparison of abundance estimates before and after subsampling.

Submodel and coefficient	Full data		Subsample	
	Sillet et al	DSM	Pre-varprop	Post-varprop
Abundance				
Chaparral	1.43 (0.229)	1.44 (0.209)	3.77 (6.403)	2.56 (9.17)
Chaparral ²	-0.38 (0.115)	-0.38 (0.126)	-0.98 (5.143)	-1.74 (6.541)
Elevation	-0.23 (0.146)	-0.23 (0.148)	-0.63 (0.49)	-0.63 (0.49)
Dispersion	0.36 (0.0777)	0.34	0.22	0.22
Detection				
Intercept	4.68 (0.0658)	4.68 (0.055)	4.23 (0.955)	4.39 (0.867)
Chaparral	-0.20 (0.060)	-0.2 (0.052)	-1.61 (2.587)	-1.14 (2.071)

Table 4: Comparison of parameter estimates from the full fall data from Sillet et al. and those using DSM, along with estimates for the subsampled data before and after our variance propagation procedure. Note that `mgcv` (and hence the `dsm` package) does not provide uncertainty around the negative binomial parameter. Intercept parameters are not comparable and therefore omitted (due to differences in how the offset is calculated in each model).

```
## Summary of uncertainty in a density surface model calculated
## analytically for GAM, with delta method
##
## Approximate asymptotic confidence interval:
##      2.5%      Mean      97.5%
##      208.649  26434.038 3348965.752
## (Using log-Normal approximation)
##
## Point estimate           : 26434.04
## CV of detection function : 0.7106491
## CV from GAM              : 21.1064
## Total standard error     : 558242.5
## Total coefficient of variation : 21.1183
```

Get corrected detection function:

```
sub_vp_ddf <- fix_ddf_vp(sub_pp)
```

A summary of the abundance results before and after variance propagation with those from the full data are given in Table 3. Comparison of model coefficients is given in Table 4.

Supplementary Material B: Simulation study

Mark V. Bravington
David L. Miller
Sharon L. Hedley

1 Introduction

To assess the properties of our proposed variance propagation method we compared results to those from assuming independence (the “delta method”) and from a one-stage fully Bayesian approach using MCMC to fit the model. We simulated data based on the island scrub jay data used as an example in the paper. Our aim here is to investigate the properties of our new method (versus the two other approaches) in the situations where the number of detections decreases. We do not concern ourselves with changing the sampling scheme or detection function covariate for simplicity of presentation and analysis. We also want to see what happens in the best possible situation, where sampler coverage is good and the only “problem” is that detectability decreases leading to a decrease in the number of animals observed. As with any set of simulations, these should not be treated as a reliable guide to performance in all conceivable situations.

2 Simulation setup

Our underlying setup was essentially the same our example for island scrub jays for fall. The underlying density of animals was `chaparral2 + chaparral + elevation` (normalized over the whole of Santa Cruz Island). We then sampled each grid cell from the prediction grid using a Poisson distribution with rate parameter a function of the underlying density, multiplied by 2500 (our target total true abundance). This lead true animal locations similar to those shown in the left panel of Figure 1. Point transect locations were left as in the example (Figure 1, right panel).

Detection functions were varied but initially based on those resulting from the fall model for island scrub jays: a half-normal detection function with chaparral as a covariate with the parameter for chaparral in the scale parameter fixed to be -0.2 throughout, the intercept parameter for the scale was varied. To decide on these parameters we effectively pursued a manual bisection on the intercept scale parameter: first using parameter values from the example analysis as a guide to parameter values to use.

Since we only wished to find out about the general performance of the procedures (rather than, say, calculate bias to a high precision), we generated 200 realizations per simulation scenario.

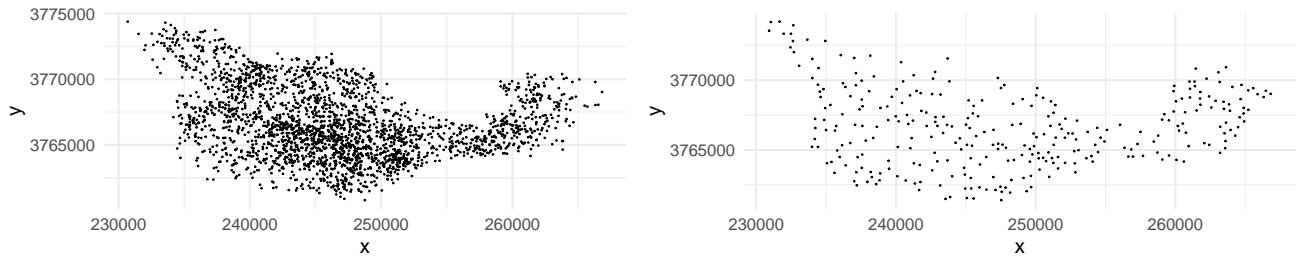


Figure 1: Left: a simulated spatial distribution used in the simulation. Right: sampler locations for the simulation study (as for the island scrub jay example).

3 Model specification

Three “models” were fitted to each data realization. In all cases, first the largest 10% of distances were discarded, this is not ideal but prevented too many simulations failing due to models overfitting to large distances (in practice one would review each model but this is clearly not possible in a simulation setting). All models used a bivariate thin plate regression spline with a basis size of 20 and assumed a Poisson distribution for the response (for simplicity).

The first two models used the `dsm` package using REML estimation. These models used the same fitted detection functions and spatial models, however one model (“delta”) used analytic estimates assuming independence between detection and spatial components whereas the other (“varprop”) used our variance propagation procedure.

The third model is rather more involved: smoothers were setup using the `mgcv::jagam` function and imported into a custom written Nimble (Valpine et al. 2017; Valpine et al. 2020) code (essentially JAGS), which included additional code for simultaneous fitting of the detection function. The spatial smoother was a thin plate spline, split into two penalties by `mgcv::jagam` to ensure priors were proper (for details see Wood 2016).

The full likelihood is the product of the detection function likelihood $(g(r_i, \sigma_i)/2\pi \int_0^w r g(r, \sigma_i) dr$, for detection i), the segment-level Poisson model and the priors on the parameters to be estimated.

Priors and intermediate calculations were set as follows:

$$\begin{aligned}
N_j &\sim \text{Poisson}(\mu_j), \\
\mu_j &= \nu_j \exp(\mathbf{X}\boldsymbol{\beta}), \\
\beta_0 &\sim N(0, \tau_{\beta_0}), \\
\boldsymbol{\beta}_{1:19} &\sim \text{MVN}(\mathbf{0}, \lambda_1 \mathbf{S}_1 + \lambda_2 \mathbf{S}_2), \\
\lambda_1, \lambda_2 &= \Gamma(0.05, 0.005), \\
\nu_j &= 2\pi \int_0^w r g(r, \sigma_j) dr, \\
g(r, \sigma) &= \exp\left(\frac{-r^2}{2\sigma^2}\right), \\
\sigma(\theta_0, \theta_{\text{chap}}, \text{chaparrel}) &= \exp(\theta_0 + \theta_{\text{chap}} \text{chaparrel}), \\
\theta_0 &\sim N(0, 0.1) \\
\theta_{\text{chap}} &\sim \text{Unif}(-2, 0).
\end{aligned}$$

where j indexes the segments and i indexes the detections. σ_j is shorthand for $\sigma(\theta_0, \theta_{\text{chap}}, \text{chaparrel}_j)$, the detection function scale parameter for segment j and σ_i is shorthand for $\sigma(\theta_0, \theta_{\text{chap}}, \text{chaparrel}_i)$, the scale parameter for detection i . MVN denotes a multivariate normal distribution parameterized by its mean vector and precision matrix and N denotes a univariate normal distribution parameterized by its mean and precision; Γ denotes a gamma distribution parameterized by its shape and rate (for consistency with Nimble code in Supplementary Materials). τ_{β_0} is the precision of the spatial model intercept (for details see Wood 2016).

We used a relatively informative prior on θ_{chap} ensuring that this parameter was negative. This was reasonable as we would expect a detectability covariate like foliage cover to be negative *a priori* (as it will decrease probability of detection). Leaving priors too vague led to abundance estimates and associated standard errors being orders of magnitude too large.

Developing the above required considerable trial-and-error and computational resources. It is difficult to come up with priors that will work reliably in a simulation setting while at the same time making the simulation fair for all models. Our experience here was that the fully Bayesian model is easy to outline but difficult to fully specify and fit (though to some extent this issue is dataset dependent). Based on these test runs and for managing computational load we selected a single chain with 500,000 iterations, with 100,000 iterations of burn-in and thinning at every 50th iteration.

All code is available as part of the Supplementary Materials.

4 Model assessment

In order to assess how well our variance propagation method performs under decreasing numbers of detections, we used a measure of “model self-confidence” which takes into account both bias and variance in the resulting estimates of total abundance. Assuming that the abundance is log-normally distributed (e.g., Buckland et al. 2001, Section 3.6), we can use a model’s estimated abundance and variance around that estimate to evaluate the quantile of that distribution that the true abundance lies in (i.e., calculate $\mathbb{P}(N_{\text{truth}} \leq \hat{N})$ for each model/simulation realization).

If our model performs perfectly then we would expect that a resulting histogram of the quantiles would be flat. Skew in the plot indicates over/under-estimation of abundance (bias). A histogram with high values at either end but a “gap” in the middle indicates uncertainty is underestimated (N_{truth} lies in the tails of the model distributions too often). A conservative estimator will give a domed histogram around 0.5, indicating intervals are too wide. The latter case seems desirable for conservation work, but a flat histogram is also acceptable. A deficiency of these plots is there is no indication of scale: one might have a very small variance but the self-confidence plot may be slightly domed or U-shaped, for this reason we also calculated the average CV for the given parameter/model combination.

For our variance propagation method and the fully Bayesian approach, we could have used posterior draws to find the quantile of N_{truth} in the posterior distribution, though this would not be possible for the delta method approach. We did test this for a subset of the simulations and found results were similar.

5 Results

Figure 2 and Table 1 summarize the results from our simulations. As we might expect, we see that performance of all methods degrades with decreasing sample size of number of detections (as mediated by the change in the detection function). The delta method is most biased in all scenarios as the model is not able to correct point estimates of detection function parameters nor estimate the covariance between the spatial model and detection function. Both our variance propagation and the one stage method perform well in the easier situations where sample size is large, with performance degrading towards bias as sample size decreases (working down Table 1 or left to right in Figure 2). The delta method gives a much smaller CV on average than either other method, with the our variance propagation method and the one stage approach giving similar results (top left corner of facets in Figure 2). Coverage of the one stage and variance propagation methods appears comparable throughout and close to nominal levels at the three higher sample sizes (Table 1, last column). Surprisingly, our variance propagation method actually performs better in terms of bias than the one-stage method in these simulations, despite the approximation involved in ours (Table 1, third column). Presumably, that somehow reflects the choices we made for priors in the one-stage method. However, as noted earlier, prior choice can be a genuine conundrum in one-stage DSMs not just for simulations but also for real-data applications, and one which our method circumvents.

References

- Buckland, S.T. et al. (2001). *Introduction to Distance Sampling: Estimating Abundance of Biological Populations*. Introduction to Distance Sampling: Estimating Abundance of Biological Populations. Oxford University Press. ISBN: 978-0-19-850649-2. URL: <https://books.google.co.uk/books?id=IVXIQgAACAAJ>.
- Valpine, Perry de et al. (Apr. 2017). “Programming with models: writing statistical algorithms for general model structures with NIMBLE”. en. In: *Journal of Computational and Graphical Statistics* 26.2. arXiv: 1505.05093, pp. 403–413. ISSN: 1061-8600, 1537-2715. DOI: 10.1080/10618600.2016.1172487. URL: <http://arxiv.org/abs/1505.05093> (visited on 07/13/2020).

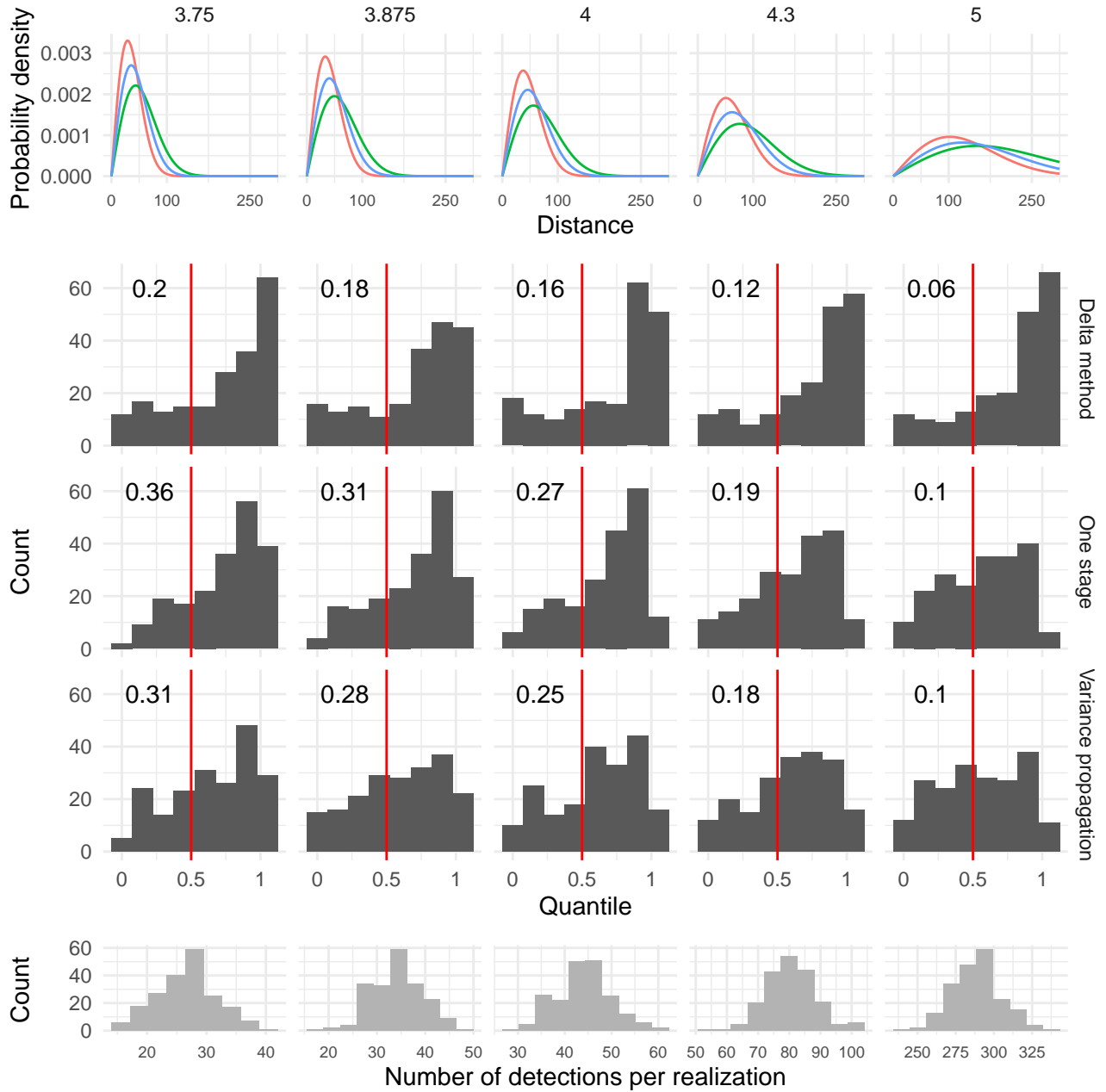


Figure 2: Top row: detection functions evaluated at different levels of chaparral (green=24, blue=47.5, red=71), top panel text gives the value of θ_0 used in the simulation, θ_{chap} was fixed to -0.2 for all simulations. Middle 3 rows: “Self-confidence” histograms showing the quantile that the true abundance lies in for each model/simulation combination. CVs (averaged over the simulations) are printed in the top left corner of each facet. Bottom row: distribution of number of detections.

Model	θ_0	Bias(\hat{N})	se(Bias(\hat{N}))	Var(\hat{N})	Var(N)	MSE	Coverage
Delta method	5.000	176.103	233.417	54776.25	2306.094	85259.71	0.635
One stage	5.000	44.657	237.591	56204.32	2306.094	57476.17	0.965
Variance propagation	5.000	22.889	261.906	68181.10	2306.094	68845.74	0.930
Delta method	4.300	305.214	419.813	176146.26	2090.242	237692.74	0.680
One stage	4.300	155.713	457.663	210850.35	2090.242	220701.52	0.940
Variance propagation	4.300	116.430	469.337	221001.83	2090.242	225429.51	0.920
Delta method	4.000	350.359	565.371	315493.80	2616.400	391315.46	0.690
One stage	4.000	277.038	601.148	356283.45	2616.400	424801.21	0.945
Variance propagation	4.000	144.868	629.705	394071.33	2616.400	404599.59	0.925
Delta method	3.875	318.274	627.819	395875.89	2482.191	462374.56	0.760
One stage	3.875	433.910	701.953	496647.78	2482.191	599028.97	0.880
Variance propagation	3.875	107.519	777.841	605445.53	2482.191	606090.59	0.870
Delta method	3.750	384.447	726.423	533489.83	2627.598	658710.47	0.690
One stage	3.750	531.775	771.133	602938.84	2627.598	828406.24	0.840
Variance propagation	3.750	247.203	846.123	721152.69	2627.598	761978.21	0.870

Table 1: Simulation results showing (per model-parameter set combination): median bias and its standard error, variance of the abundance estimate (which includes variance in the true N , which changed per simulated dataset), variance of true abundance (to give comparison to the previous column), mean squared error (MSE), and coverage (proportion of simulations where the true abundance was within the 95% interval, constructed via a log-normal approximation).

- Valpine, Perry de et al. (2020). *NIMBLE: MCMC, Particle Filtering, and Programmable Hierarchical Modeling*. URL: <https://doi.org/10.5281/zenodo.1211190>.
- Wood, Simon N. (2016). “Just Another Gibbs Additive Modeler: Interfacing JAGS and mgcv”. en. In: *Journal of Statistical Software* 75.7. ISSN: 1548-7660. DOI: 10.18637/jss.v075.i07. URL: <http://www.jstatsoft.org/v75/i07/> (visited on 01/25/2018).

Supplementary Material C: Asymptotic properties of the approximation used for variance propagation

Mark V. Bravington
David L. Miller
Sharon L. Hedley

The purpose of this Supplementary Material is to show that our approximation does not worsen the asymptotic performance when estimating smoother coefficients β or the variance/smoothing-related hyperparameters ω , compared to an "idealized REML" alternative that would (somehow) still use Laplace Approximation to estimate ω but without the approximations related to the detection probabilities. We assume that the problem is sufficiently regular for standard asymptotics to apply (for example: parameter estimates not on the boundary; priors that support the truth, etc; see e.g. Pfanzagl 1973 and Weng 2010), and in particular so that the use of a smoother can be justified in the first place (Wood, Pya, and Säfken 2016).

A further complication arises in the detection function/density surface setting. For the detection function parameters θ , the number of sightings $n = \sum y_i$ constitutes the sample size, and is an ancillary statistic that in itself carries no information about θ (though it does affect the precision). However, n itself is a random variable that is directly affected by β in the density surface (in particular, by the intercept β_0). A more relevant asymptotic quantity for the density surface would be total survey effort A , corresponding to overall area searched. Here we assume that A would be increased by replicating the segments. In practice, of course, available survey effort tends to be used not to repeat segments but rather to infill between existing ones, so that the design points X_i become increasingly dense but are not replicated; however, asymptotic arguments are much simpler in the repeated case.

Our goal here is not statistical rigour per se, but rather to highlight the comparative importance of terms included and excluded in our approximation. Therefore, we make a number of simplifications at the loss of generality, in particular by treating the detection function parameter as if it were one-dimensional, and assuming that the count data are Poisson; those assumptions do not affect the flow of the logic, but do considerably simplify the algebra. The additivity property of Poisson distributions means that increasing the "sample size" (by repeating segments) has the same statistical effect as simply increasing the search effort within each segment. Therefore we can keep the number of segments fixed in the algebra, and write instead

$$\begin{aligned}\mu_i &\triangleq \mathbb{E}[Y_i] \\ \log \mathbb{E}[Y_i] &= \log A + q_i(\theta) + X_i^\top \beta\end{aligned}$$

and deal with asymptotics as $A \rightarrow \infty$. The number of sightings n , on which inferences about detection-function parameters θ are based, is $O_p(A)$, and for any i we have $\mathbb{E}[Y_i] = O_p(A)$ and $\mathbb{V}[Y_i] = O_p(A)$.

Below we use standard formulae for Poisson distributions, in this form

$$\begin{aligned}\log f(y|\mu_i) &= C + y_i \log \mu_i - \mu_i \\ \frac{d\mu_i}{d\beta} &= X_i \mu_i \\ \frac{d\mu_i}{d\delta} &= \frac{d\mu_i}{d\theta} = q'_i \mu_i\end{aligned}$$

where the "constant" C varies from line to line.

We further assume that detection function estimation takes place in a Bayesian context, leading to a detection posterior $f_n(\theta)$. (In practice, MLE will often be used, implicitly corresponding to a weak prior.) We assume an Edgeworth-like expansion for f_n , centred on the detection posterior mode $\hat{\theta}$. While such expansions are routine in MLE settings, the Bayesian setting entails more algebra and some extra regularity conditions, basically to ensure that the influence of the Bayesian prior is asymptotically negligible; see eg Weng (2010). The expansion nevertheless has the familiar form, given in eqn (52) of that paper. In the one-dimensional case used here for simplicity, it can be written as

$$\begin{aligned}f_n(\theta) &= \sqrt{v} \times \varphi\left(\frac{\delta}{\sqrt{v}}\right) \times \left(1 + O(n^{-1/2}) \text{poly}_2\left(\frac{\delta}{\sqrt{v}}\right)\right) \\ \implies \log f_n(\theta) &= \frac{1}{2} \log v - \frac{\delta^2}{2v} + O(n^{-1/2}) \text{poly}_2\left(\frac{\delta}{\sqrt{v}}\right)\end{aligned}$$

where $\delta = \theta - \hat{\theta}$, $v = \mathbb{V}[\theta|s] = O(n^{-1})$, $\varphi(\cdot)$ is a standardized Gaussian PDF, and $\text{poly}_2(x)$ is a polynomial with leading term in x^2 formed from Hermite polynomials; the term in x^1 must vanish, because the expansion is centred on the mode $\delta = 0$ where $d \log f_n(\theta) / d\theta = 0$. Replacing v by an estimate \hat{v} (the detection posterior variance) does not affect the order of asymptotic expansion that we will require. Standard asymptotic results are that $\delta = O_p(n^{-1/2})$, $v = O_p(n^{-1})$, $\delta/\sqrt{v} = O_p(1)$. Because $n = O_p(A)$, we also have e.g. $\delta^2 = O_p(A^{-1})$, etc.

Conditional on smoothing parameters ω and detection data s , the joint log-density of the counts y , the smoother coefficients β , and the detection parameters θ is

$$\begin{aligned}\Lambda &\triangleq \log f(y, \beta, \theta|s) \\ &= C + \sum (y_i \log \mu_i - \mu_i) - \frac{1}{2} \beta^\top W \beta + \log f_n(\theta) \\ &= \sum y_i \log A + \sum y_i (q_i(\theta) + \beta^\top X_i) - A \sum \exp(q_i(\theta) + \beta^\top X_i) - \frac{1}{2} \beta^\top W \beta + \log f_n(\theta) \\ &= C + \sum y_i (q_i + \beta^\top X_i) - A \sum \exp(q_i + \beta^\top X_i) - \frac{1}{2} \beta^\top W \beta - \frac{\delta^2}{2v} + O(n^{-1/2}) \text{poly}_2\left(\frac{\delta}{\sqrt{v}}\right)\end{aligned}\tag{0.1}$$

where W is the prior precision matrix for β . Our approximation $\tilde{\Lambda}$ omits the higher-order terms in f_n and uses a linear approximation to q , to give

$$\begin{aligned}\tilde{\mu}_i &= A \exp(\hat{q}_i + \hat{q}'_i \delta + \beta^\top X_i) \\ \tilde{\Lambda} &= C + \sum (y_i \log \tilde{\mu}_i - \tilde{\mu}_i) - A \sum \exp(\hat{q}_i + \hat{q}'_i \delta + \beta^\top X_i) - \frac{1}{2} \beta^\top W \beta - \frac{\delta^2}{2v}\end{aligned}\tag{0.2}$$

Since $q_i = \hat{q}_i + \hat{q}'_i \delta + \frac{1}{2} \hat{q}''_i \delta^2 + O(\delta^3)$, we have

$$\begin{aligned} \exp(\hat{q}_i + \hat{q}'_i \delta + \beta^\top X_i) &= \exp(q_i + \beta^\top X_i - \frac{1}{2} \hat{q}''_i \delta^2 + O(\delta^3)) \\ &= \exp(q_i + \beta^\top X_i) \exp(-\frac{1}{2} \hat{q}''_i \delta^2 + O(\delta^3)) \\ &= \exp(q_i + \beta^\top X_i) (1 - \frac{1}{2} \hat{q}''_i \delta^2 + O(\delta^3) + O(\delta^4)) \\ &= \exp(q_i + \beta^\top X_i) + (-\frac{1}{2} \hat{q}''_i \delta^2 + O(\delta^3)) \exp(q_i + \beta^\top X_i) \\ &\implies \tilde{\mu}_i = \mu_i (1 - \frac{1}{2} \hat{q}''_i \delta^2 + O(\delta^3)) \end{aligned}$$

and thus we can write eqn (0.2) as

$$\begin{aligned} \tilde{\Lambda} &= C + \sum y_i (q_i - \frac{1}{2} \hat{q}''_i \delta^2 + O(\delta^3) + \beta^\top X_i) - A \sum \exp(q_i - \frac{1}{2} \hat{q}''_i \delta^2 + O(\delta^3) + \beta^\top X_i) \\ &\quad - \frac{1}{2} \beta^\top W \beta - \frac{\delta^2}{2v} - O(n^{-1/2}) \text{poly}_2\left(\frac{\delta}{\sqrt{v}}\right) \\ &= C + \sum (y_i \log \mu_i - \mu_i) + \sum y_i (-\frac{1}{2} \hat{q}''_i \delta^2 + O(\delta^3)) - A \sum (-\frac{1}{2} \hat{q}''_i \delta^2 + O(\delta^3)) \exp(q_i + \beta^\top X_i) - O(n^{-1}) \\ &= \Lambda + \sum (y_i - \mu_i) (-\frac{1}{2} \hat{q}''_i \delta^2 + O(\delta^3)) - O(n^{-1/2}) \text{poly}_2\left(\frac{\delta}{\sqrt{v}}\right) \end{aligned}$$

Inference is determined not by Λ and Λ' directly, but rather for their derivatives WRTO β and δ , for which we have:

$$\frac{d\tilde{\Lambda}}{d\beta} = \frac{d\Lambda}{d\beta} - \sum X_i \mu_i (-\frac{1}{2} \hat{q}''_i \delta^2 + O(\delta^3)) \quad (0.3)$$

$$\frac{d\tilde{\Lambda}}{d\delta} = \frac{d\Lambda}{d\delta} - \sum \hat{q}'_i \mu_i (-\frac{1}{2} \hat{q}''_i \delta^2 + O(\delta^3)) + \sum (y_i - \mu_i) (-\hat{q}'_i \delta + O(\delta^2)) - \frac{1}{\sqrt{v}} O(n^{-1/2}) \text{poly}_1\left(\frac{\delta}{\sqrt{v}}\right) \quad (0.4)$$

The leading term in

$$\frac{d\Lambda}{d\beta} = \sum X_i (y_i - \mu_i) - \beta^\top W$$

is a random variable with mean 0 and variance $O(A)$, and thus has typical magnitude $O(A^{1/2})$. This dominates the term $\beta^\top W$ which is $O(1)$, so we can write

$$\frac{d\Lambda}{d\beta} = O_p(A^{1/2})$$

and, by comparison, the second term in eqn (0.3) is $O_p(A) \times O_p(A^{-1}) = O_p(1)$ where the factor $O_p(A)$ comes from μ_i , and the factor $O_p(A^{-1})$ is the asymptotic magnitude of δ^2 . Consequently, $d\Lambda/d\beta = O_p(A^{1/2})$ and our approximation $d\tilde{\Lambda}/d\beta$ differs from it by a term only of $O_p(1)$.

$$\begin{aligned} \frac{d\Lambda}{d\beta} &= O_p(A^{1/2}) \\ \frac{d\tilde{\Lambda}}{d\beta} &= \frac{d\Lambda}{d\beta} + O_p(1) \\ &= \frac{d\Lambda}{d\beta} (1 + O_p(A^{-1/2})) \end{aligned} \quad (0.5)$$

For δ , we have

$$\begin{aligned} \frac{d\Lambda}{d\delta} &= O_p(A^{1/2}) \\ \sum q'_i \mu_i \left(-\frac{1}{2} \hat{q}''_i \delta^2 + O(\delta^3)\right) &= O(A) \times O(A^{-1}) = O_p(1) \\ \sum (y_i - \mu_i) \left(-\hat{q}''_i \delta + O(\delta^2)\right) &= O_p(A^{1/2}) \times O_p(A^{-1/2}) = O_p(1) \\ \frac{1}{\sqrt{v}} O(n^{-1/2}) \text{poly}_1\left(\frac{\delta}{\sqrt{v}}\right) &= O_p(A^{-1})^{-1/2} \times O_p(A^{-1/2}) \times O_p(1) = O_p(1) \end{aligned}$$

so that again

$$\begin{aligned} \frac{d\Lambda}{d\delta} &= O_p(A^{1/2}) \\ \frac{d\tilde{\Lambda}}{d\delta} &= \frac{d\Lambda}{d\delta} + O_p(1) \\ &= \frac{d\Lambda}{d\delta} (1 + O_p(A^{-1/2})) \end{aligned} \tag{0.6}$$

Writing $\psi \triangleq (\beta, \delta)$ and extending the computations to second order shows that

$$\begin{aligned} \frac{d^2\Lambda}{d\psi^2} &= O_p(A) \\ \frac{d^2\tilde{\Lambda}}{d\psi^2} &= \frac{d^2\Lambda}{d\psi^2} + O_p(A^{1/2}) \end{aligned} \tag{0.7}$$

Now, writing $\Lambda(\psi; y)$ to emphasize the dependence on count data, the ideal posterior mode $\hat{\psi}$ satisfies

$$\Lambda'(\hat{\psi}; y) \triangleq \left. \frac{d\Lambda}{d\psi} \right|_{\hat{\psi}} = 0$$

whereas our approximation finds $\tilde{\psi}$ such that

$$\tilde{\Lambda}'(\tilde{\psi}; y) \triangleq \left. \frac{d\tilde{\Lambda}}{d\psi} \right|_{\tilde{\psi}} = 0$$

The equations leading up to (0.7) show that $\tilde{\Lambda}$ is an asymptotically small perturbation of Λ of order $O(A^{-1/2})$ compared to Λ itself, and that the same holds for the derivatives. Hence it is natural to expect that the difference in the roots $\tilde{\psi} - \hat{\psi}$ should also be asymptotically small compared to $\hat{\psi}$. The fact that $\tilde{\psi}$ and $\hat{\psi}$ are defined implicitly rather than explicitly makes a formal proof cumbersome, but here we sketch an approach based on Taylor expansions around the true value ψ_0 . We take $\psi_0 = 0$ WLOG, and for convenience write $\Lambda_0 \triangleq \Lambda(0; y)$ and replace tensor expressions such as $\psi^\top \Lambda''_0$ by their scalar equivalents such as $\psi \Lambda''_0$, etc, so that

$$\Lambda'(\psi) = \Lambda'_0 + \psi \Lambda''_0 + O(\psi^2)$$

Since $\hat{\psi} = O_p(A^{-1/2})$ by standard arguments, the terms in ψ^2 and higher become asymptotically negligible near the root $\hat{\psi}$ compared to terms in ψ^0 and ψ^1 , so that

$$\Lambda'(\hat{\psi}) = 0 \implies \hat{\psi} = -\left(\frac{\Lambda'_0}{\Lambda''_0}\right) + O_p(A^{-1})$$

A formal development would entail multivariate series inversion; see e.g. Barndorff-Nielsen and Cox 1989, section 6.10.

For the approximate solution $\tilde{\psi}$, the analogous expression is

$$\tilde{\psi} = -\left(\frac{\tilde{\Lambda}'_0}{\tilde{\Lambda}''_0}\right) + O_p(A^{-1})$$

Finally, we can substitute from eqns (0.5) and (0.6) so that

$$\begin{aligned} \tilde{\psi} &= -\left(\frac{\Lambda'_0(1 + O_p(A^{-1/2}))}{\Lambda''_0(1 + O_p(A^{-1/2}))}\right) + O_p(A^{-1}) \\ &= -\left(\frac{\Lambda'_0}{\Lambda''_0}\right)(1 + O_p(A^{-1/2})) + O_p(A^{-1}) \\ &= \hat{\psi} + O_p(A^{-1}) \end{aligned}$$

The point here is that the posterior mode of $\tilde{\Lambda}$ is close to the posterior mode of the ideal Λ , i.e. to order $O(A^{-1})$, and a similar argument applies to the Hessian. Since the Laplace Approximation on which REML estimates of hyperparameters involves only the mode and the Hessian, the same accuracy should apply to hyperparameter estimates, and then to inference about β conditional on hyperparameters. And since Laplace Approximations themselves are generally valid to $O(n^{-1})$ (Tierney and Kadane 1986), there is no loss of asymptotic order from the approximations we propose. In contrast, though, the derivations above show that naive estimates of β and ω based on treating the detection posterior mode $\hat{\theta}$ as exact, i.e. fixing $\delta = 0$ and neglecting even the first-order terms in δ which our approximation does include, would be of lower asymptotic accuracy.

References

- Barndorff-Nielsen, O. E. and D. R. Cox (1989). *Asymptotic Techniques for Use in Statistics*. Chapman and Hall.
- Pfanzagl, J. (1973). “The accuracy of the normal approximation for estimates of vector parameters”. In: *Zeitschrift für Wahrscheinlichkeitstheorie und Verwandte Gebiete* 25, pp. 171–198.
- Tierney, Luke and Joseph B. Kadane (1986). “Accurate Approximations for Posterior Moments and Marginal Densities”. In: *Journal of the American Statistical Association* 81.393, pp. 82–86. DOI: 10.1080/01621459.1986.10478240.
- Weng, R.C. (2010). “A Bayesian Edgeworth expansion by Stein’s identity”. In: *Bayesian Analysis* 5, pp. 741–763.
- Wood, Simon N., Natalya Pya, and Benjamin Säfken (2016). “Smoothing Parameter and Model Selection for General Smooth Models”. In: *Journal of the American Statistical Association* 111.516, pp. 1548–1563. DOI: 10.1080/01621459.2016.1180986. URL: <https://doi.org/10.1080/01621459.2016.1180986>.